NASA Technical Memorandum 86882

Studies on the Hot Corrosion of a Nickel-Base Superalloy—Udimet 700

Ajay K. Misra
Lewis Research Center
Cleveland, Ohio

November 1984

NASA

STUDIES ON THE HOT CORROSION OF A NICKEL-BASE SUPERALLOY - UDIMET 700*

Ajay K. Misra†
National Aeronautics and Space Administration
Lewis Research Center
Cleveland, Ohio 44135

SUMMARY

The hot corrosion of a nickel-base superalloy, Udimet 700, has been studied in the temperature range of 884 to 965 °C and with different amounts of Na_2SO_4. Two different modes of degradation were identified: (1) formation of Na_2MoO_4 - MoO_3 melt and fluxing by this melt, (2) formation of large interconnected sulfides. The present studies have shown that the dissolution of Cr_2O_3, TiO_2 in the Na_2SO_4 melt does not play a significant role in the overall corrosion process. The conditions for the formation of massive interconnected sulfides were identified and a mechanism of degradation due to sulfide formation is described. The formation of Na_2MoO_4 - MoO_3 melt requires an induction period and various physicochemical processes during the induction period were identified. The factors affecting the length of the induction period were also examined. From the present studies, the melt penetration through the oxide appears to be the prime mode of degradation whether the degradation is due to the formation of sulfides or the formation of the Na_2MoO_4 - MoO_3 melt.

INTRODUCTION

Na_2SO_4 is the prime constituent of the deposit on the blades and first stage guide vanes in combustion gas turbines. The superalloys and coating systems used in the gas turbines suffer from accelerated corrosion known as hot corrosion in the presence of a molten Na_2SO_4 deposit. Various mechanisms (refs. 1 to 6) have been proposed to explain the hot corrosion process and these can be broadly divided into two categories; (1) the fluxing process, and (2) the sulfidation mechanism. The fluxing mechanism was first proposed by Bornstein and DeCrescente (ref. 1) and Goebel and Pettit (refs. 2 and 3). The fluxing mechanism involves dissolution of the protective oxides in the melt at the melt-oxide interface with subsequent reprecipitation at the melt-gas interface. The dissolution of oxides is basic or acidic, depending on the Na_2O activity in the melt. Basic dissolution occurs for high Na_2O activities in the melt, and in the mechanism of Goebel et al. (refs. 2 and 3), high Na_2O activities are generated in the melt by introduction of sulfides in the alloy. However, for a limited amount of Na_2SO_4, the melt would saturate with the products of basic dissolution and the basic fluxing is only of transient in nature. On the other hand, the dissolution is acidic for low Na_2O activities in the melt. In the mechanism, proposed by Goebel and Pettit (ref. 3), acidic fluxing is observed for alloys containing the refractory elements (Mo, W). The Na_2O activity is lowered by the addition of the oxides of the refractory elements (MoO_3, WO_3) to the melt, and acidic fluxing can be self-sustaining, thus resulting in catastrophic corrosion. Fryburg et al. (ref. 4) have studied the

*Work funded under NASA Grant NCC 3-43.

†Case Western Reserve University, Dept. of Metallurgy and Materials Science, Cleveland, Ohio and NASA Lewis Resident Research Associate.

hot corrosion of a molybdenum containing nickel-base superalloy and their studies have led to a mechanism different than that of Goebel and Pettit (ref. 3). According to the mechanism, proposed by Fryburg et al. (ref. 4), all the Na_2SO_4 was converted to Na_2MoO_4 before the onset of catastrophic corrosion and corrosion took place by a Na_2MoO_4 - MoO_3 melt. A detailed mechanism of corrosion by the Na_2MoO_4 - MoO_3 melt has been described by the present author (ref. 7). Rapp and Goto (ref. 8) have described the criterion for sustained fluxing beneath a thin salt film, according to which the solubility gradient must be negative across the melt from the melt-oxide to the melt-gas interface. Various fluxing processes have been examined in detail by Shores (ref. 9) and he concluded that sustained fluxing can take place only for a limited number of cases. In most of the cases, fluxing would be transient in nature.

Besides fluxing, the other important role of the Na_2SO_4 melt is to introduce sulfur into the alloy, thus forming the internal sulfides. The mechanism, by which sulfides are introduced into the alloy, is not clear yet. Simons et al. (ref. 5) have proposed that sulfides are formed by reduction of the Na_2SO_4 melt by an unspecified reducing agent. The presence of carbon in the deposit is known to cause sulfide formation by reducing the Na_2SO_4 melt to Na_2S (ref. 10), The sulfides, once formed, can lead to accelerated corrosion. The accelerated corrosion occurs by preferential oxidation of the sulfides, and the sulfur, released by the preferential oxidation, is conserved in the alloy. This has been the basis of the sulfidation - oxidation mechanism, as has been described by Spengler and Viswanathan (ref. 11). Goebel and Pettit (ref. 12) have studied the oxidation behavior of presulfidised nickel-base alloys and observed that the oxidation rate of presulfidised Ni - Cr alloys was affected by sulfur, only when liquid nickel sulfides were present along with chromium sulfides. However, in many instances, the morphology produced by the oxidation of the presulfidised alloys shows remarkable similarity to the hot corroded alloys (ref. 13). This has led many investigators to believe that the prime role of Na_2SO_4 is to introduce sulfur into the alloy.

The corrosion of superalloys also depends upon the particular testing method employed. Two different testing procedures are usually employed to study the hot corrosion of superalloys. One is the laboratory salt-spray tests, in which a limited amount of Na_2SO_4 is sprayed onto the samples before being oxidized at high temperatures. The second is the high velocity burner rig tests, in which the Na_2SO_4 is continuously deposited onto the samples, which are exposed to high velocity, high-temperature gases. The burner rig tests are usually closer to the actual engine operations. The agreement between the laboratory and burner rig tests are generally varied. For the molybdenum containing nickel base superalloys, there are large differences between the laboratory and burner rig test results. In the laboratory tests, a fluxing type of scale morphology is observed, in which Mo plays a distinct role and corrosion takes place by a Na_2MoO_4 - MoO_3 melt (refs. 4 and 14). On the other hand, in the burner rig tests, the fluxing due to the molybdenum content of the alloy is not observed and a sulfidation-oxidation type of morphology is usually observed (refs. 15 and 16). In both the laboratory and burner rig tests, an induction period is observed before the onset of accelerating corrosion. However, the physicochemical processes during the induction period are not well characterized.

The present work has been undertaken to study in detail the hot corrosion of a nickel-base superalloy, Udimet 700. This alloy was chosen because of its intermediate hot corrosion resistance. The particular interest in the present

studies is to determine the conditions under which various hot corrosion mechanisms are operative. The effect of various parameters like the amount of Na_2SO_4, and temperature on the hot corrosion of Udimet 700 has also been studied.

EXPERIMENTAL PROCEDURE

The alloy used is Udimet 700, which is a wrought nickel-base superalloy. The composition of the alloy is given in table I. The test samples were coupons, approximately of size 23.5 by 10.8 by 2.4 mm with a hangdown hole in one end. All surfaces were glass head blasted to give an uniform surface finish. The coupons were cleaned ultrasonically in trichloroethylene, detergent, distilled water and alcohol and then dried in an oven at 120 °C. The samples were coated with Na_2SO_4 by airbrushing a saturated solution of salt onto the coupons, which were heated on a hot plate to 200 °C. The corrosion experiments were performed in a vertical tube furnace. The flow of oxygen was downward at 100 cm min^{-1}. Continuous gravimetric measurements were made with a microbalance. The temperature range of interest in the present studies is 884 to 965 °C. The test samples, corroded for different lengths of time were washed in hot distilled water and the solutions were analyzed for various water soluble elements. For a few experiments the concentration of SO_2 in the gas flowing out of the furnace tube was measured during the test. The SO_2 was measured continuously with a thermoelectron pulsed fluorescent SO_2 analyzer. The corroded samples were examined by conventional metallography and electron-optical techniques.

RESULTS

General features of corrosion. - The general features of corrosion kinetics are shown in figure 1, which is the kinetics for U-700, coated with 3.5 mg/cm^2 Na_2SO_4 and corroded at 950 °C. The details of the corrosion kinetics will be shown in later sections. The kinetics, in general, can be divided into three different periods, (1) an initial period, during which there is a rapid increase in the weight gain of the sample, (2) an induction period, during which small overall weight gains are observed, and (3) a period of accelerating corrosion, during which large weight gains are observed and the corrosion is catastrophic. The weight gains during the period of accelerating corrosion are much higher than that during the initial period of corrosion. The length of each period in the corrosion kinetics and the total weight gain or the extent of corrosion during each period are strong functions of the amount of Na_2SO_4 and temperature, which will be described in later sections. In some cases, the length of the initial period is 2 to 3 hr, whereas in other cases, the length of the initial period is 40 to 50 hr. Similarly, the length of the induction period in some cases is 2 to 3 hr, whereas in other cases, it is 200 to 300 hr.

The samples, corroded for different lengths of time were washed in hot distilled water and the solution was analyzed for various chemical elements like Na, SO_4, Mo, Cr, Ni and Co. No significant amounts of Ni and Co were detected in the waterwashed solution. The SO_4 and Cr in the solution are due to the presence of Na_2SO_4 and Na_2CrO_4 respectively. The Mo in the solution is due to the presence of Na_2MoO_4 and MoO_3 in the corrosion product layer. Figure 2 shows the amounts of various species, in millimoles as a function of

time for a sample, coated with 3.5 mg/cm^2 Na_2SO_4 and corroded at 950 °C. The SO_4 content of the melt decreases from the beginning and reaches a zero value at the end of the initial period. The SO_4 content remains at the near zero value throughout the induction period. The beginning of the period of accelerating corrosion is marked by the slow rise in the SO_4 content of the solution. During the period of accelerating corrosion, the SO_4 content of the solution rises slowly, reaches a peak and then decreases again. The Cr content of the solution increases during the initial period, and attains a maximum value at the end of the initial period. The Cr content of the solution decreases during the induction period and attains a near zero value at the beginning of the period of accelerating corrosion. There is a sharp increase in the Mo content of the solution during the initial period, followed by a slow increase during the induction period. The beginning of the period of accelerating corrosion is marked by a rapid increase in the Mo content of the solution.

The SO_2 evolved as a function of time for a sample, coated with 3.5 mg/cm^2 Na_2SO_4 and corroded at 950 °C is shown in figure 3. At the beginning of the corrosion experiment, there is a sudden increase in the SO_2 evolved and the increase continues for about half an hour. After about half an hour, the SO_2 evolution starts to decrease until the end of the initial period, at which a near zero value is obtained. Throughout the induction period, the SO_2 evolution remains at the near zero value until the beginning of the period of accelerating corrosion. The SO_2 evolution increases during the period of accelerating corrosion, reaches a peak and decreases with further progress of time.

Initial period of corrosion. - In the corrosion kinetics shown in figure 1, the initial period is shown as a linear curve, however, the nature of the corrosion kinetics during the initial period is more complex and is very much dependent on the amount of Na_2SO_4 and temperature. Figure 24 shows the kinetics during the first four hours of corrosion during the initial period for U-700, coated with different doses of Na_2SO_4 at 950 °C. At 950 °C, the corrosion kinetics during the first 2-1/2 to 3 hr is the same for all the doses of Na_2SO_4. At the start of the corrosion experiment, there is a rapid increase in the weight gain, followed by a slowing down in the rate of corrosion. The sample gains weight at a slower rate until about 1 hr. At about 1 hr after the beginning of the corrosion experiment, there is a sudden increase in the rate of weight gain. This is similar to the breakaway oxidation observed in many cases of alloy oxidation (ref. 17). The rapid weight gain or the breakaway oxidation continues for about 1 to 1-1/2 hr. After this, the rate of weight gain slows down. For amounts of $Na_2SO_4 \leq 2$ mg/cm^2, the slowing of the rate of weight gain marks the beginning of the induction period. However, for the heavier doses of Na_2SO_4, after about 3 hr from the start of the corrosion experiment, there is again a sudden increase in the rate of weight gain. The sample starts to gain weight at a linear rate. For convenience, the sudden increase in the rate of weight gain after 1 hr of the start of the corrosion experiment will be called the first breakaway oxidation and that observed after 3 hr from the start of the corrosion experiment will be called the second breakaway oxidation.

For the heavier doses of Na_2SO_4, the sample does not continue to gain weight at a linear rate for an indefinite period after the second breakaway oxidation period. Rather, the rate of weight gain slows down again. However, several periods of breakaway oxidation can be observed during the initial period for the heavy doses of Na_2SO_4, and this is shown in figure 5. After each breakaway oxidation period, a linear rate of weight gain is observed for

some time. The rate during the linear period was observed to be nearly the same for all the doses of Na_2SO_4 ($\approx$0.8 mg/cm^2-hr) and is shown in table II. After several breakaway oxidation periods in the initial period, the rate of weight gain slows down and this marks the beginning of the induction period. It will be seen later that breakaway oxidations are also observed during the induction period. However, the rate of weight gain during the breakaway oxidations in the induction period is much smaller than that during the initial period. The total weight gain at the end of the initial period is a strong function of the amount of Na_2SO_4, and this relationship at 950 °C is shown in figure 6. For doses up to about 2 mg/cm^2 Na_2SO_4, the total weight gain at the end of the initial period remains constant and for doses >2mg/cm^2 Na_2SO_4, the total weight gain at the end of the initial period increases with an increase in the amount of Na_2SO_4 and a linear relationship is observed.

The scale morphology of samples corroded for different lengths of time up to the end of the first breakaway oxidation period in the initial corrosion kinetics is shown in figure 7. It must be noted that the scale morphology is the same irrespective of the amount of Na_2SO_4. After 15 min of corrosion, a thin scale is produced, which is composed of primarily Cr, Al, Ti oxides, and a few discrete internal sulfide particles are also found in the cross section (fig. 7(a)). At the very beginning of first breakaway oxidation period in the initial corrosion kinetics, the scale morphology shows a continuous layer of interconnected internal sulfides at the scale-metal interface and some unoxidized alloy in between these sulfides (fig. 7(b)). Beneath the layer of interconnected internal sulfides are the discrete sulfide particles. The sulfides were observed to be Cr, Al, and Ti, however, the detailed composition of the sulfides was not determined. The scale morphology towards the end of the first breakaway oxidation period (after about 2 hr at 950 °C) shows a distinct band of internal oxides and some unoxidized alloy in between the internal oxides (fig. 7(c)). The internal oxides appear to have been formed by the oxidation of the internal sulfides, and at a few places, the sulfides can be seen to be in contact with the internal oxides. The internal oxides are Cr, Al, and Ti oxides. Beneath the zone of internal oxides is a region consisting of discrete internal sulfides. Few large sulfide particles can be seen in figure 7(c), however, most of the sulfides are discrete and they are not in contact with the internal oxide scale. The presence of the internal discrete Cr, Ti sulfides also depletes the matrix of these alloying elements. For the small and intermediate doses of Na_2SO_4 (up to about 2 mg/cm^2) for which no second breakaway oxidation period was observed in the initial corrosion kinetics, the unoxidized areas in between the internal oxides are oxidized with further progress of time and the resulting scale morphology is shown in figure 8. Note that the thickness of the external scale in figure 8 is nearly the same as the thickness of the external scale plus the internal oxidation region in figure 7(c). For low and intermediate doses of Na_2SO_4, the scale morphology essentially remains the same throughout the induction period.

For the heavy doses of Na_2SO_4 (7$\approx$2 mg/cm^2), the scale morphology up to the end of the first breakaway oxidation period is the same as that shown in figure 7. For the heavy doses, the kinetics shows a second breakaway oxidation period during the initial period. The scale morphology at the very beginning of the second breakaway oxidation is shown in figure 9. Beneath the external scale, massive internal sulfides are formed. The sulfides are very large and these large sulfides are interconnected among themselves and also in contact with the external scale. X-ray maps show these sulfides to be composed of Cr, Ti and this leaves the unoxidized region in between to consist of Ni, Co, and

Mo only. Beneath the zone of large interconnected internal sulfides, a few discrete internal sulfide particles are observed. It must be noted that the large interconnected sulfides are formed almost instantaneously: the scale morphology at half an hour before the beginning of the second breakaway oxidation is similar to that shown in figure 7(c).

The kinetics shows a linear rate of weight gain after the second breakaway oxidation period for the heavier doses and the typical scale morphology during this period of linear weight gain is shown in figure 10. A part of the massive interconnected internal sulfides have oxidized to their respective oxides. Beneath the zone of interconnected internal sulfides, there is a thick zone of discrete internal sulfide particles. A comparison of the scale morphology in figure 10 to that at the beginning of the second breakaway oxidation period (fig. 9) shows a considerable increase in the thickness of the zone of discrete internal sulfide particles. The scale morphology towards the end of the initial period for the heavy doses of Na_2SO_4 is shown in figure 11. It can be seen that all the massive network of internal sulfides have oxidized by now. Also some of the unoxidized alloy in between the internal sulfide network have oxidized by now. However, some unoxidized areas in between the internal oxide network are still present. There is a band of internal sulfides at the scale-metal interface and the details of the scale-metal interface at a higher magnification (fig. 11(b)) shows some internal sulfides to be quite large. Some of the internal sulfides are interconnected among themselves, however, none of the sulfides are connected to the external scale.

The top surface of the samples, corroded for different lengths of time at 950 °C, is shown in figures 12 and 13. After 15 min of corrosion at 950 °C, the top surface consists of a melt (Na_2SO_4 - Na_2CrO_4) with some oxide needles protruding through it (fig. 12(a)). The oxide needles are TiO_2, as determined from the EDAX analysis. At one place, the melt spalled off on cooling and a layer of oxide can be seen beneath the melt. After 30 min of corrosion at 950 °C, the melt can be seen on the top surface of the scale (fig. 12(b)), however, by now parts of the oxide grains can be seen above the melt. The morphology, shown in figure 12(b) suggests that the oxides are immersed in the melt, with a part of the oxide on the top of the melt. The morphology of the top surface after 1 hr of corrosion at 950 °C is shown in figure 13. The top surface has spalled off at several locations. The details of the top surface at a location, where the oxide has not spalled off, is shown in figure 13(b). The top surface in figure 13(b) shows oxide grains and melt penetration through it. Note that the melt is not present as a continuous layer over the oxide anymore. The magnified view of the top surface, where the outer oxide layer has spalled off, shows a very porous layer (fig. 13(c)). It must be noted that 1 hr in the corrosion kinetics corresponds to the time period after the first breakaway oxidation period. The study of the morphology of the top surfaces shows that there is gradual melt penetration through the oxide underneath it.

Figure 14 shows the details of the increase in Cr content of the water-washed solution as a function of time during the initial period for a sample, coated with 3.5 mg/cm^2 Na_2SO_4 and corroded at 950 °C. At the beginning of the corrosion experiment, the Cr content of the solution increases rapidly, and it slows down after the initial rapid rise. After about 45 min of corrosion, there is a sharp and sudden increase in the Cr content of the solution. After the sudden increase, the Cr content of the melt increases at a slower rate until about 3 hr. At this time, there is again a sudden increase in the Cr content of the solution, followed by a slow increase in the Cr content with

progress of time. It is worth noting that the times, at which the sudden increase in the Cr content of the solution occurs, corresponds to the beginning of the breakaway oxidation periods. The time of 45 min corresponds to the beginning of the first breakaway period, where as the time of 3 hr corresponds to the beginning of the second breakaway oxidation period. Also note that the increase in the Cr content of the solution at the beginning of the second breakaway oxidation period is higher than that at the beginning of the first breakaway oxidation period.

The general features of the corrosion kinetics during the initial period are the same for all the temperatures. However, the time required for the second breakaway oxidation to occur and large interconnected sulfides to form increases with a decrease in temperature, and this is shown in figure 15 for four different temperatures. At 950 °C, it takes 3 hr for the second breakaway oxidation to occur, whereas it takes 7 hr and 12 to 13 hr for the second breakaway oxidation to occur at 920 °C and 900 °C respectively. As seen in figure 15(a), no distinction could be made between the first and second breakaway oxidation periods at 965 °C.

Induction period. - The induction period is the time period, during which the weight gains are relatively small. Figure 16 shows the details of the induction period for the low and intermediate doses of Na_2SO_4. From figure 16, several breakaway oxidation periods can be observed at frequent intervals during the induction period. The average rates of weight gain during these breakaway oxidation periods are observed to be 0.1 mg/cm^2-hr at 950 °C. Note that this rate is much smaller than that observed during the breakaway oxidation period in the initial corrosion kinetics. After each breakaway oxidation period in the induction period, the rate of weight gain is similar to that observed in the pure oxidation of U-700. For low and intermediate doses of Na_2SO_4, the average rate of weight gain during induction period (including that during the breakaway oxidation periods) was observed to be of the order of 0.04 mg/cm^2-hr. For heavier doses of Na_2SO_4 ($7 \approx 2$ mg/cm^2), breakaway oxidation periods could not be observed during the induction period. The average rate of weight gain during the induction period for the heavier doses of Na_2SO_4 increases with an increase in the amount of Na_2SO_4 and this is shown in table III.

For low and intermediate doses of Na_2SO_4, there is no change in scale morphology during the induction period. For the heavier doses of Na_2SO_4, the scale morphology during the induction period is shown in figure 17. A comparison of the scale morphology shown in figure 17 to that in figure 11(c) (the scale morphology at the end of the initial period) shows that most of the unoxidized areas in between the internal oxides in figure 11 have oxidized by now. The most significant differences in the scale morphologies at the end of the initial period and that during the induction period are the morphologies of the internal sulfides. In the scale morphology at the end of the initial period (fig. 11), the sulfides were discrete particles and uniformly present throughout the alloy beneath the zone of internal oxides. However, with the progress of time, there is a change in the sulfide morphology and the sulfides are primarily concentrated along the alloy grain boundaries (fig. 17).

The length of the induction period is observed to be a strong function of the amount of Na_2SO_4 and the relationship at 950 °C is shown in figure 18. The length of the induction period increases with an increase in the amount of Na_2SO_4, reaches a peak, and then decreases with further increase in the amount

of $NaSO_4$. For amounts of Na_2SO_4 greater than about 4 mg/cm^2, the length of the induction period remains constant. Similar relationship between the length of the induction period and the amount of Na_2SO_4 is obtained at all the temperatures and table IV shows the length of the induction period versus the amount of Na_2SO_4 at 900 °C. Although, the general trend is the same, for the same amount of Na_2SO_4, the length of the induction period is increased considerably at 900 °C. For example, for a dose of 1.47 mg/cm^2 Na_2SO_4, the length of the induction period was observed to be of the order of 300 hr at 900 °C as compared to 45 to 50 hr at 950 °C.

Period of accelerating corrosion. - From chemical analysis (fig. 2), it was seen that the onset of the period of accelerating corrosion is associated with a rapid rise in the Mo content of the melt. A typical scale morphology at the end of the period of accelerating corrosion is shown in figure 19. The pitting type of corrosion morphology is observed and the pit consists of a Na_2MoO_4 - MoO_3 melt. A thick outer porous oxide layer (NiO + Cr_2O_3) had spalled off from the surface. The sulfides have disappeared from the scale morphology. The presence of sulfides in the scale morphology for the heavier doses of Na_2SO_4 causes SO_2 evolution during the period of accelerating corrosion, which is due to the oxidation of the sulfides. The evolution of SO_2 also converts a part of Na_2MoO_4 to Na_2SO_4 and this causes a rise in the SO_4 content of the water washed solution during the period of accelerating corrosion. The total amount of SO_2 evolved during the period of accelerating corrosion increases with an increase in the amount of Na_2SO_4 and this is shown in table V.

DISCUSSION

In the hot corrosion of U-700, two different modes of degradation are clearly evident. One mode of degradation involves formation of a Na_2MoO_4 - MoO_3 melt and rapid corrosion by this melt. This mode of degradation occurs for all the doses of Na_2SO_4, however, the time required for the degradation by Na_2MoO_4 - MoO_3 melt to occur is a strong function of the amount of Na_2SO_4 and temperature. The second mode of degradation is due to the formation of massive internal interconnected sulfides. This mode of degradation occurs for the heavier doses of Na_2SO_4 and takes place during the initial period.

Degradation due to the formation of sulfides. - First consider the degradation process due to the formation of massive interconnected sulfides. The mechanism of formation of massive sulfides will be discussed later in this section. Spengler and Viswanathan (ref. 11) have described a mechanism, according to which the degradation occurs by the preferential oxidation of the sulfides, thus releasing further sulfur into the alloy. Release of sulfur into the alloy causes the formation of more sulfides. In this way sulfur is conserved in the alloy and this has been the basis for the sulfidation - oxidation mechanism, as described by Spengler and Viswanathan (ref. 11). In the present studies, massive interconnected internal sulfides were observed in the scale morphology just at the beginning of the second breakaway oxidation period in the initial corrosion kinetics. After this, a linear rate of weight gain is obtained. It must be noted that the formation of sulfides by itself does not contribute to any weight gain, since the sulfur comes from the Na_2SO_4 applied to the samples. The scale morphology during the linear weight gain period after the beginning of second breakaway oxidation shows preferential oxidation of sulfides

(fig. 10). However, the total weight gain during this period of weight gain cannot be accounted for by the preferential oxidation of sulfides only. For example, for a dose of 3.5 mg/cm^2 Na_2SO_4, the maximum amount of sulfur that can be introduced in the alloy is 0.788 mg/cm^2. Assuming all the sulfides are Cr_2S_3, the oxidation reaction for the sulfides can be written as

$$Cr_2S_3 + \frac{3}{2} O_2 = Cr_2O_3 + \frac{3}{2} S_2 \qquad (1)$$

Assuming that all the sulfur is conserved in the alloy, the maximum O_2 pick up due to the oxidation of all the sulfides would be 0.788 mg/cm^2. Similarly, assuming that all the sulfides are CrS, the maximum oxygen pick up would be 0.591 mg/cm^2. The weight gain, as determined from the kinetics, represent the O_2 pick up and therefore the preferential oxidation of sulfides, by itself, cannot account for the total weight gain during the second breakaway oxidation for the heavier doses (about 5 mg/cm^2 for a dose of 3.5 mg/cm^2 Na_2SO_4).

The rapid weight gains observed after the formation of massive sulfides can be explained as follows. As seen in the scale morphology in figure 9, the sulfides are interconnected among themselves and also in contact with the external scale. The formation of the network of interconnected Cr, Ti sulfides depletes the alloy region in between these sulfides of Cr and Ti. The external scale is porous and the examination of the top surface has shown the melt to be dispersed in the oxide. The large internal sulfides, that are in contact with the external scale, are oxidized. The oxidation of sulfides would generate a porous oxide scale. Thus O_2 can come in contact with the regions in between the sulfides, which consist of primarily Ni, Co, and Mo. Rapid oxidation of the depleted region in between the internal sulfides takes place and this results in large weight gains after the second breakaway oxidation period.

According to the sulfidation - oxidation mechanism, proposed by Spengler and Viswanathan (ref. 11), it would appear that once the sulfide are formed, the corrosion would continue for an indefinite period. In the present study, this does not appear to be the case as regards the weight gains are concerned. This is reflected in the fact that the linear rate of weight gain after the second breakaway oxidation in the initial corrosion kinetics for the heavier doses does not continue for an indefinite period. The rate of weight gain rather slows down and this leads to the induction period. The studies on the corrosion kinetics in the presence of a Na_2SO_4 - Na_2CrO_4 melt might be complicated by any effect that the melt might have on the corrosion kinetics. Therefore, to verify independently that the formation of massive sulfides does not lead to a linear period of weight gain for an indefinite period, the following experiment was performed. A U-700 sample was coated with 5.7 mg/cm^2 Na_2SO_4 and corroded at 950 °C up to the time corresponding to the beginning of the second breakaway oxidation in the initial period of corrosion. After this, the sample was taken out of the furnace and hot washed in distilled water to remove any melt that is present in the scale. The washed sample was reoxidized again at 950 °C. Figure 20 shows the kinetics after reoxidation at 950 °C. The rate of weight gain is linear up to about 4 mg/cm^2 of weight gain, after which the rate slows down. After about 10 hr, the rate becomes similar to that of oxidation of U-700 in O_2 only (without the salt deposit) and a near parabolic rate is obtained. The rate of weight gain during the linear period is of the order of 0.8 mg/cm^2-hr, which is the same as that shown in table II for corrosion by the Na_2SO_4 melt. This further confirms that after the second breakaway oxidation, the rate of weight gain is not affected by the presence of the melt. During

the reoxidation experiment at 950 °C, the SO_2 coming out of the furnace tube was continuously monitored and the SO_2 evolution as a function of time is also shown in figure 20 along with the kinetics. There is some SO_2 evolution during the linear weight gain period, suggesting some loss of sulfur to the atmosphere due to the oxidation of sulfides.

The slowing of the rate of weight gain after the linear period is due to a change in the morphology of the internal sulfides. It appears that the oxidation of the interconnected sulfide network produces discrete sulfides beneath the region of interconnected sulfides. The reasons for this are not clear and is a subject of further investigation in this laboratory. Based on the scale morphologies observed in the present study, a generalized model for the oxidation of the internal sulfide network is proposed. The schematics of the oxidation of interconnected sulfide network are shown in figure 21 and is described in detail as follows.

(1) At the beginning of the linear weight gain period, the interconnected sulfide network is in contact with the porous external scale (fig. 21(a)).

(2) With passage of time, a part of the sulfides adjacent to the external scale is oxidized along with the alloy region surrounding this area of the sulfide. Some of the sulfur, released due to the oxidation of the sulfides diffuse through the alloy and form discrete sulfide particles beneath the zone of interconnected sulfide network (fig. 21(b)).

(3) With further progress of time, more of the interconnected sulfides and the alloy surrounding it are oxidized, thus releasing more sulfur into the alloy. Some new discrete sulfide particles are formed, and growth of some of the old discrete sulfide particles takes place. Due to the growth of some of the old sulfide particles, a few large sulfide particles are produced beneath the zone of interconnected sulfide network (fig. 21(c)).

(4) With further progress of time, all the interconnected sulfides adjacent to the external scale oxidizes. Due to the further release of sulfur into the alloy, the growth of the existing sulfide particles takes place and few large sulfide particles come in contact with the oxidized sulfide network (fig. 21(d)).

As mentioned earlier, the linear rate of weight gain after the formation of large interconnected sulfides is due to the preferential oxidation of the sulfides and the depleted alloy in between these sulfides. The preferential oxidation of sulfides and the alloy in between these sulfides requires supply of O_2, and if the sulfides are in direct contact with the porous external scale or the porous oxidized sulfide layer, O_2 can readily be supplied. If all the new sulfides, that are produced by the oxidation of the old sulfides, are in direct contact with the porous external scale, then a linear rate of weight gain would continue indefinitely. The oxidation of sulfides, that are not in contact with the external scale or the oxidized sulfide layer, would require transport of O_2 through the alloy and this situation is similar to that of internal oxidation. This would result in a slower rate of weight gain. Thus, for the hot corrosion situation, the linear period of weight gain after the second breakaway oxidation in the initial corrosion kinetics is due to the preferential oxidation of sulfides formed at the beginning of the breakaway oxidation period and the oxidation of the alloy in between the sulfides. After oxidation of all the sulfides in the sulfide network, that was formed in

the beginning of the second breakaway oxidation period, the area of the new sulfides that are in contact with the oxidized sulfide layer is very small (fig. 21(d)). This results in a reduction in the rate of weight gain. Although there is a reduction in the rate of weight gain, it is still faster than that of pure oxidation in O_2. This is due to the gradual oxidation of the alloy areas in between the oxidized sulfides. Also, the internal discrete sulfide particles oxidize, the oxygen being supplied by the diffusion of O_2 through the alloy. Again, further sulfur is released into the alloy. The scale morphology during the induction period (fig. 17) shows that with progress of time, the discrete sulfide particles are preferentially segregated along the alloy grain boundaries. The reasons for the change in sulfide morphology from that of uniform discrete particles to preferential segregation along the grain boundaries is not clear and is a subject of further investigation in this laboratory.

From the above discussion, the degradation due to sulfide formation can be divided into two categories:

(1) Overall consumption of metal due to the preferential oxidation of the sulfides and the depleted alloy region surrounding the sulfides. This mode of degradation occurs when large internal interconnected sulfides are in direct contact with the porous external scale.

(2) Internal penetration of sulfur along the alloy grain boundaries deep inside the alloy. This mode of degradation occurs after the large interconnected sulfides are completely oxidized. This does not contribute to any significant metal wastage. However, the segregation of sulfides along the grain boundaries might have detrimental effect on the mechanical properties of the superalloy (ref. 18).

Mechanism of sulfide formation. - Two different types of sulfide morphologies are produced. One is the discrete sulfide particles and the second is the massive interconnected internal sulfides. In terms of material degradation, the formation of massive internal interconnected sulfides is detrimental and therefore it is instructive to examine the conditions leading to the formation of these massive sulfides. A mechanism of sulfide formation beneath a Na_2SO_4 melt has been described by Goebel et al. (ref. 3). According to this mechanism a layer of oxide, e.g., Cr_2O_3 or Al_2O_3 is developed beneath the Na_2SO_4 melt. Some of the oxygen required for the formation of oxides come from the Na_2SO_4 melt, thus resulting in an oxygen potential gradient across the melt. The lowering of the P_{O_2} at the oxide melt interface would cause the P_{S_2} to go up at this interface.[2] The sulfur diffuses through the oxide lattice to the metal oxide interface, where P_{O_2} is low, thereby forming the internal sulfides.

The kinetics and the scale morphology obtained during the hot corrosion of U-700 does not support the above mechanism because of the following factors. (1) Large interconnected sulfides are formed almost instantaneously. This is seen both in the scale morphology and in the corrosion kinetics. In the kinetics, the interconnected sulfide formation is marked by the beginning of a breakaway oxidation in the initial period. According to the mechanism of Goebel et al. (ref. 3), the introduction of sulfur would be gradual, since it involves diffusion of sulfur through the compact scale. (2) A compact scale is never observed beneath the melt. The oxide scale is porous and the morphology shows melt penetration through the oxide.

In the light of the above discussions, a mechanism is proposed to describe the formation of sulfides which is as follows. The sulfides are formed in the alloy only when the Na_2SO_4 melt comes in direct contact with the alloy. The melt can come in direct contact with the alloy by penetration through the oxide layer, which was clearly evidenced in the morphology of the top surfaces. The mechanism by which sulfides are formed by direct contact of the melt with the alloy is the reduction of $SO_4^{=}$. The reduction reaction of $SO_4^{=}$ as seen described by Fang and Rapp (ref. 19), which is described by the following:

$$SO_4^{=} + 4e^{-} = S^{2-} + 2O_2^{2-} \qquad (2)$$

The electrons are supplied by the metal oxidation reaction. ($M \rightarrow M^{n+} + Ne^{-}$). S^{2-} ions are produced by the reduction reaction, thus causing the formation of sulfides. When the Na_2SO_4 melt comes in contact with an alloy containing various alloying elements like Cr, Ti, Al , the extent of sulfidation and the morphology of the internal sulfides appear to be dependent on the concentration of the alloying elements. The scale morphology suggests that large interconnected sulfides are formed only when the alloy beneath the melt is depleted of the alloying elements like Cr, Ti. This is explained in detail as follows.

When the alloy, U-700, comes in contact with the melt at the beginning of the corrosion experiment, few discrete sulfide particles are formed in the first few minutes of corrosion and an external scale consisting of $Cr_2O_3 + TiO_2$ is developed. The presence of discrete sulfide (Cr, Ti Sulfides) particles depletes the matrix of Cr and Ti. However, at the beginning of the experiment only few discrete sulfide particles are formed, and the distance to which they extend into the alloy is very small. Thus, the extent of depletion would be relatively mild and the thickness of the depletion zone is also relatively small. With the passage of time, the melt penetration through the outer oxide layer occurs, and after some time the melt comes in contact with the depleted region, and large interconnected sulfides are formed. This marks the beginning of the first breakaway oxidation period in the initial corrosion kinetics. However, the thickness of the depletion region was small and the extent of depletion was relatively mild. Thus the extent of formation of interconnected sulfide network is small. During the first breakaway oxidation period, the interconnected sulfide and the alloy in between the sulfides oxidize. In the previous section, it was mentioned that the oxidation of the interconnected sulfide network produces small and discrete sulfide particles beneath the zone of interconnected sulfides. The new sulfides formed are small and distributed in a near uniform manner throughout the alloy, whereas, the sulfides in the interconnected network are large in size. Thus, the area occupied by the new small sulfide particles is larger than that occupied by the interconnected sulfide network. Therefore, the thickness of the depletion region beneath the external scale and the internal oxide is greater than that formed in the first few minutes of corrosion. After the first breakaway oxidation period, when the melt again penetrates the layer of oxide/internal oxides and touches the alloy surface, the melt comes in contact with a thick depleted region of the alloy. This results in formation of large interconnected internal sulfides as seen at the beginning of the second breakaway oxidation period.

A comparison of the total weight gain during the breakaway oxidation periods shows that the total weight gain during the second breakaway oxidation period is greater than that during the first breakaway oxidation period. This is due to the formation of higher amount of interconnected sulfides at the

beginning of the second breakaway oxidation period as compared to that at the beginning of the first breakaway oxidation. Again, this is clearly related to the differences in the extent of depletion and the thickness of the depleted zone. A detailed investigation is underway to examine the effect of the alloy content on the formation of interconnected sulfides. Preliminary results (ref. 20) show that in lower Cr containing alloys, large interconnected sulfides are formed at the beginning of the corrosion experiment. On the other hand, for the higher Cr containing alloys, large interconnected sulfides are formed only after a few breakaway oxidation periods and only if Na_2SO_4 is available for a longer time.

Role of dissolution of oxides by Na_2SO_4 during the initial period of corrosion. - The primary oxides formed in the oxidation of U-700, as determined in a separate study by the author, are Cr_2O_3 + TiO_2 with a few internal Al_2O_3 stringers. The reaction of Na_2SO_4 with Cr_2O_3 and TiO_2 can be described as

$$Na_2SO_4 + Cr_2O_3 + \frac{3}{4} O_2 = Na_2CrO_4 + SO_3 \quad (3)$$

$$Na_2SO_4 + nTiO_2 = (Na_2O)nTiO_2 + SO_3 \quad (4)$$

The compound Na_2CrO_4 is water soluble and $(Na_2O)nTiO_2$ is not water soluble. Results of the chemical analysis during the initial period (fig. 14) shows that large amounts of Na_2CrO_4 are formed immediately after the beginning of the breakaway oxidation periods. During other times, there is only slow increase in the Na_2CrO_4 content of the melt. The sharp rise in the Na_2CrO_4 content of the melt at the beginning of the breakaway oxidation period is due to the formation of sulfides at the beginning of this period, which is explained as follows. It was previously mentioned that the sulfides are formed by reduction of the sulfate with the metal. Removal of sulfur from the melt increases the Na_2O activity of the melt. The reaction of Na_2SO_4 with Cr_2O_3 is greatly enhanced by the increase in the Na_2O activity. The increase in Na_2O activity due to sulfide formation would be dependent on the amount of sulfur removed from the melt by the sulfate reduction reaction. At the beginning of the second breakaway oxidation, greater amounts of sulfides are formed as compared to that at the beginning of the first breakaway oxidation period. Thus, the Na_2O activity at the beginning of the second breakaway oxidation period is higher than that at the beginning of the first breakaway oxidation period. This would result in greater amount of Na_2CrO_4 to be formed at the beginning of the second breakaway oxidation period than that at the beginning of the first breakaway oxidation.

Large amount of Na_2CrO_4 are formed only when sulfides are formed in the alloy by direct reaction of the melt with the alloy. During the other times, the formation of Na_2CrO_4 takes place at a slower rate suggesting that reaction of neutral Na_2SO_4 with Cr_2O_3 is a slower process. The sharp rise in the Na_2CrO_4 content of the melt at the beginning of the breakaway oxidation periods further confirms that the sulfides are formed almost instantaneously and breakaway oxidation starts after their formation.

It must be recognized that the large weight gains during the initial period of corrosion are due to the formation of large sulfides and subsequent oxidation of these sulfides along with the alloy in between the sulfides. The formation of large amounts of Na_2CrO_4 at the beginning of the breakaway oxidation period is only incidental to the sulfide formation and not the primary cause of corrosion. During other times, the reaction between Na_2SO_4 and Cr_2O_3

is slow and does not appear to have significant effect on the overall corrosion process. The melt penetration through the oxides appear to be more important than the dissolution of oxides by the melt. This is also true for the hot corrosion of other superalloys and various coating systems, which has been investigated by the present author in a separate study (ref. 20).

Sulfide formation as a function of the amount of Na_2SO_4. - From the mechanisms of sulfide formation, it is seen that sulfides are formed by direct interaction of the melt with the alloy. Thus, formation of sulfides requires the presence of Na_2SO_4 in the melt. This is also further confirmed by the chemical analysis of the corroded samples during the initial period for low and intermediate doses of Na_2SO_4. Table VI shows the SO_4 content of the water washed solution for low and intermediate doses of Na_2SO_4 after 2-1/2 hrs of corrosion at 950 °C and it can be readily seen that most of the Na_2SO_4 had been converted to other sodium compounds. This is the reason why no second breakaway oxidation period was observed in the corrosion kinetics during the initial period for low and intermediate doses of Na_2SO_4. Table VII shows that for the heavier doses of Na_2SO_4, all the Na_2SO_4 is not converted to other Na compounds even 1 hr after the beginning of the second breakaway oxidation period. A comparison of the amount of Na_2SO_4 reacted after 4 hr of corrosion at 950 °C (this time corresponds to 1 hr after the beginning of the second breakaway oxidation period) shows the amount of Na_2SO_4 reacted to be the same for all the doses of Na_2SO_4. This is to be expected because (1) most of the conversion of Na_2SO_4 takes place at the very beginning of the breakaway oxidation periods and (2) the extent of sulfidation at the beginning of the breakaway oxidation period is dependent on the extent of alloy depletion plus the thickness of the depleted zone, but not on the amount of Na_2SO_4.

The formation of all the sulfides at the beginning of the breakaway oxidation period is instantaneous and after this the melt is in contact with the sulfides underneath it. The scale morphology shows the sulfides to be very compact and free of pores. Thus, further contact of the melt with the depleted alloy would take place after the oxidation of all the sulfides. After the oxidation of all the interconnected sulfide network, the melt can penetrate through the oxidized sulfide layer and thus come in contact with the depleted alloy region, resulting in formation of more sulfides. This is seen in the corrosion kinetics having more than two periods of breakaway oxidation during the initial corrosion kinetics. Except for the beginning of the breakaway oxidation period, the conversion of Na_2SO_4 to Na_2CrO_4 or other Na compounds is a slower process. Thus, most of the Na_2SO_4, that is still present in the melt after few minutes of breakaway oxidation, will be conserved until the beginning of the next breakaway oxidation. This process would continue until all the Na_2SO_4 had been converted to Na_2CrO_4 and other Na compounds. Therefore the total amount of sulfides formed during the initial period would increase with an increase in the amount of Na_2SO_4. No analysis of the total sulfur content of the alloy as a function of the amount of Na_2SO_4 was made. However, it will be seen later that during the period of accelerating corrosion, all the sulfides oxidize, thus releasing SO_2 into the atmosphere. Thus, the total amount of SO_2 evolved during the period of accelerating corrosion, which was shown in table V, would give an indication about the amount of sulfides formed. From table V, it is seen that the total amount of SO_2 evolved during the period of acceleraing corrosion increases with an increase in the amount of Na_2SO_4. This further confirms that the total amount of sulfides formed in the alloy increases with an increase in the amount of Na_2SO_4. Since the degradation in the initial period of corrosion is due to the formation of sulfides, the total

weight gain or the extent of material loss at the end of the initial period of corrosion increases with an increase in the amount of Na_2SO_4. The initial period comes to an end when all the Na_2SO_4 has been converted to other Na compounds and no more new sulfides can be formed. This was reflected in the chemical analysis of the waterwashed solutions, shown in figure 2, in which the SO_4 content of the solution attains a near zero value at the end of the initial period.

Physicochemical processes during the induction period. - From the chemical analysis of the waterwashed solutions, it is known that the end of induction period is marked by the conversion of most of the Na_2CrO_4 to Na_2MoO_4. An induction period also has been observed for corrosion of U-700 by a Na_2MoO_4 melt (ref. 21) and it has been shown that the period of accelerating corrosion begins after the overall MoO_3 content of the melt assumes a certain minimum value. The conversion of Na_2CrO_4 to Na_2MoO_4 also requires addition of MoO_3 to the melt. Thus, during the induction period, MoO_3 is added to the melt. In an alloy consisting of Ni, Co, Cr, Ti, Al, Mo (about 2.8 at % Mo), MoO_3 can be formed by two different ways: (1) During the transient period of oxidation, when a fresh alloy surface comes in contact with the oxidant, the oxides of all the elements of the alloy including Mo are formed on the surface. (2) If the alloy is depleted in the alloying element like Cr, Ti, Al and the matrix consists of Ni, Co, and Mo only, then MoO_3 can be formed.

Formation of an internal network of interconnected sulfides depletes the areas in between these sulfides of Cr, Ti, and these areas primarily consist of Ni, Co and Mo. During the breakaway oxidation period, the oxidation of the areas in between the sulfides takes place, resulting in formation of some MoO_3. This can be readily seen in figure 22, which shows that there is a sharp increase is the Mo content of the waterwashed solution during the first breakaway oxidation period in the initial corrosion kinetics. Similar results would be anticipated during all the breakaway oxidation periods, which are due to the formation of the interconnected sulfides. During the induction period several breakaway oxidation periods are observed at frequent intervals in the corrosion kinetics. However, the average rate of weight gain during the breakaway periods in the induction period are much smaller than the initial period. This is due to the fact that all the Na_2SO_4 has been converted to other Na compounds by the end of the initial period. Thus during the breakaway oxidations in the induction period, the melt that comes in contact with the alloy does not contain any Na_2SO_4. Therefore sulfides are not formed at the beginning of the breakaway oxidations in the induction period and large weight gains are not observed. However, during each breakaway oxidation in the induction period, fresh alloy surface is oxidized, resulting in formation of some MoO_3 during the transient period.

At 950 °C, for very small doses of Na_2SO_4 ($\approx$0.5 mg/cm^2), the MoO_3 formed during the first breakaway oxidation may be enough to convert all the Na_2SO_4 and Na_2CrO_4 to Na_2MoO_4 and thus form a Na_2MoO_4 - MoO_3 melt at the end of the first breakaway oxidation period. Indeed, this is the case at 950 °C for the lowest dose of Na_2SO_4 ($\approx$0.5 mg/cm^2), and is shown in figure 23. The period of accelerating corrosion starts immediately after the first breakaway oxidation period in the initial corrosion kinetics and no distinct induction period was observed. At 950 °C, for doses of Na_2SO_4 greater than 0.5 mg/cm^2, the MoO_3 added during the first breakaway oxidation period is not enough to convert all the Na_2SO_4 to Na_2CrO_4 and Na_2MoO_4 and form a Na_2MoO_4 - MoO_3 mixture. Therefore

more MoO_3 has to be added to the melt before the onset of the period of accelerating corrosion. For low and intermediate doses of Na_2SO_4, for which no second breakaway oxidation period in the initial corrosion kinetics was observed (i.e., no extensive interconnected sulfide network is formed during the initial period), addition of MoO_3 takes place primarily during breakaway oxidation periods in the induction period. Assuming that the amount of MoO_3 added to the melt during each breakaway oxidation in the induction period is the same always, then the number of breakaway oxidations required for the formation of a Na_2MoO_4 - MoO_3 melt would increase with an increase in the amount of Na_2SO_4. This is seen in figure 24, which compares the details of the corrosion kinetics for two different doses of Na_2SO_4. From the above considerations, an increase in the length of the induction period with an increase in the amount of Na_2SO_4 would be expected for low and intermediate doses of Na_2SO_4.

In general, the amount of sulfides formed are seen to increase with an increase in the amount of Na_2SO_4. Thus, there are two competing factors which determine the length of the induction period:

(1) The amount of MoO_3 to be added to the corrosion product layer for the formation of a Na_2MoO_4 - MoO_3 melt increases with an increase in the amount of Na_2SO_4.

(2) The amount of interconnected network of sulfides formed increases with an increase in the amount of Na_2SO_4, thus facilitating the formation of MoO_3 by oxidation of alloys in between the sulfides. Therefore, because of the above two competing factors, a maximum in the length of the induction period would be observed at a certain dose of Na_2SO_4 (as shown in fig. 18).

Period of accelerating corrosion. - During the period of accelerating corrosion, the corrosion takes place by a Na_2MoO_4 - MoO_3 melt. The mechanism of corrosion by a Na_2MoO_4 - MoO_3 melt has been described by the present author (ref. 7). Briefly, the MoO_3 is formed at the melt-gas interface by the Mo^{+4}/Mo^{+6} exchange reaction in the melt. Mo^{+6} migrates from the melt-gas to the melt-alloy interface and Mo^{+4} migrates from the melt-alloy to the melt-gas interface. At the melt-alloy interface, oxidation of Ni to Ni^{++} takes place by reaction with Mo^{+6} and the Ni^{++} is transported to the melt-gas interface, where it is converted to NiO. Besides the above reactions, the basic fluxing of Cr_2O_3 and Al_2O_3 by the melt also takes place.

During the period of accelerating corrosion, the overall consumption of the alloy by the Na_2 MoO_4 - MoO_3 melt takes place. Due to this the sulfides are oxidized, thus releasing SO_2 to the atmosphere. This causes the evolution of SO_2 during the period of accelerating corrosion for the heavier doses of Na_2SO_4 (fig. 3).

Effect of temperature on the overall corrosion process. - The general features of corrosion, e.g., kinetics and the scale morphology are the same at all the temperatures. However, the major effect of temperature is to increase the length of the induction period with a decrease in temperature. Also, for the heavier doses, the time for the beginning of second breakaway oxidation in the initial period increases with a decrease in temperature. Since the breakaway oxidation periods involve melt penetration through the oxide scale and contact of the melt with the alloy, it is apparent that the temperature has a major effect on the melt penetration through the oxide. One possible effect of temperature is to increase the viscosity of the melt with a decrease in temperature and thus affecting the wetting properties of the oxide. For a viscous

melt, the melt penetration through the oxide would be more difficult and it might take a longer time for the melt to penetrate a layer of oxide.

SUMMARY AND CONCLUSION

In the hot corrosion studies on U-700, two primary modes of degradation were observed; (1) degradation due to formation of large network of sulfides. (2) formation of Na_2MoO_4 - MoO_3 melt and fluxing by the Na_2MoO_4 - MoO_3 melt. An induction period was observed before the degradation by Na_2MoO_4 - MoO_3 melt occurs and the length of the induction period was observed to be a strong function of the amount of Na_2SO_4 and temperature. The results from the present studies have shown that the fluxing is only important in the case of corrosion by the Na_2MoO_4 - MoO_3 melt. Again, even in the case of corrosion by Na_2MoO_4 - MoO_3 melt, the fluxing does not take place by the conventional dissolution and reprecipitation of oxides. Rather, the fluxing takes place by a Mo^{+4}/Mo^{+6} exchange reaction in the melt, and the oxidation of Ni to Ni^{++} at melt-alloy interface. The Ni^{++} is transported through the melt and at the melt-gas interface, NiO is formed.

Rapid dissolution of Cr_2O_3 is observed at the beginning of the breakaway oxidations in the initial period of corrosion. However, it must be emphasized that the rapid dissolution of Cr_2O_3 is incidental to the formation of sulfides and not the cause of the sulfide formation. During other times, the dissolution of Cr_2O_3 in the Na_2SO_4 melt is a slower process, and does not contribute significantly to the corrosion process. Frequently, melt penetration through the oxide occurs and this was marked by several periods of breakaway oxidation both during the initial period and the induction period. Indeed, the penetration of the melt through the oxide should be considered as the primary mode of degradation, because (1) both discrete sulfides and large interconnected sulfides are formed by the direct contact of the Na_2SO_4 melt with the alloy and (2) MoO_3, required for the formation of the Na_2MoO_4 - MoO_3 melt, is formed by the oxidation of a fresh alloy surface during the breakaway oxidation period.

The degradation due to the formation of large interconnected sulfides involves preferential oxidation of the sulfides and the alloy in between the sulfides, thus resulting in an overall material consumption. During the oxidation process, the morphology of the sulfides changes from that of large interconnected sulfides to that of small and discrete particles. With further progress of time, the sulfides are preferentially concentrated along the alloy grain boundaries. In terms of overall material degradation, the formation of large interconnected sulfides is detrimental. The interconnected sulfides are formed by the direct contact of the Na_2SO_4 melt with the Cr depleted region in the alloy.

One important factor that is evident from the present studies is the importance of testing conditions, particularly the amount of Na_2SO_4. For example, if a test was undertaken at 900 °C with a dose of 0.5 mg/cm^2 Na_2SO_4, then the alloy would undergo catastrophic corrosion in 10 to 15 hrs due to the formation of a Na_2MoO_4 - MoO_3 melt. However, if a test is undertaken at 900 °C with a dose of 1.5 mg/cm^2 Na_2SO_4, the alloy undergoes catastrophic corrosion only after about 300 hr of testing time. The dose of 1.5 mg/cm^2 also is not enough for the formation of large interconnected sulfides. Thus the tests with a dose of 1.5 mg/cm^2 Na_2SO_4 for times shorter than 300 hr would conclude that there is less corrosion with an increase in the amount of Na_2SO_4. Again, for

the heavy doses of Na_2SO_4, at 900 °C, the degradation of the alloy takes place in the first 15 to 20 hr due to a different mechanism, e.g., the formation of large interconnected sulfides. From these considerations, it is obvious that erroneous conclusions would be obtained about hot corrosion resistance of the superalloy if tests were carried out with a single dose of Na_2SO_4.

REFERENCES

1. Bornstein, N.S.; and DeCrescente, M.A.: The Role of Solium in the Accelerated Oxidation Phenomenon Termed Sulfidation. Metall. Trans., vol. 2, no. 10, Oct. 1971, pp. 2875-2883.

2. Goebel, J.A.; and Pettit, F.S.: Na_2SO_4 - Induced Accelerated Oxidation (Hot Corrosion) of Nickel. Metall. Trans., vol. 1, no. 7, July 1970, pp. 1943-1954.

3. Goebel, J.A.; Pettit, F.S.; and Goward, G.W.: Mechanisms for the Hot Corrosion of Nickel-Base Alloys. Metall. Trans., vol. 4, no. 1, Jan. 1973, pp. 261-278.

4. Fryburg, George C., et al: Chemical Reactions Involved in the Initiation of Hot Corrosion of B-1900 and NASA-TRW VIA. J. Electrochem. Soc, vol. 129, no. 3, Mar. 1982, pp. 571-585.

5. Simons, E.L.; Browning, G.V.; and Liebhafsky, H.: Sodium Sulfate in Gas Turbines. Corrosion, vol. 11, no. 12, Dec. 1955, pp. 17-25.

6. Stringer, J.; Role of Sulfur in Hot Corrosion. Proceedings of Gas Turbine Materials in the Marine Environment, John W. Fairbanks and Irvine Machlin, eds., MCIC-75-27, Metals and Ceramics Information Center, 1975, pp. 161-182.

7. Misra, A.K.: Mechanism of Na_2SO_4 Induced Corrosion of Molybdenum Containing Nickel Base Superalloys at High Temperatures. I. Corrosion in Atmospheres Containing O_2 Only. Submitted for publication in the Journal of the Electrochemical Society.

8. Rapp, Robert A.; and Goto, K.S.: The Hot Corrosion of Metals by Molten Salts. Proceedings of the Second International Symposium on Molten Salts, Jerry Braunstein and J. R. Selman, eds., Electrochemical Society, 1981, p. 159.

9. Shores, D.A.; New Perspectives on Hot Corrosion Mechanisms. High Temperature Corrosion, Robert A. Rapp, ed., National Association of Corrosion Engineers, 1983, p. 493.

10. McKee, D.W.; and Romeo, G.: Effects of Transient Carbon Deposition on the Sodium Sulfate-Induced Corrosion of Nickel-Base Alloys. Metall. Trans. A, vol. 6, no. 1, Jan. 1975, pp. 101-108.

11. Spengler, C.J.; and Viswanathan, R.: Effect of Sequential Sulfidation and Oxidation on the Propagation of Sulfur in an 85 Ni-15 Cr Alloy. Metall. Trans., vol. 3, no. 1, Jan. 1972, pp. 161-166..

12. Goebel, J.A.; and Pettit, F.S.: The Influence of Sulfides on the Oxidation Behavior of Nickel-Base Alloys. Metall. Trans., vol. 1, no. 12, Dec. 1970, pp. 3421-3429.

13. El-Dahshan, M.E.; Whittle, D.P.; and Stringer, J.: Effect of Presulfidation on the Oxidation Behavior of Co-Based Alloys. Part I. Presulfidation at Sulfur Partial Pressures Above the Dissociation Pressure of Cobalt Sulfide. Oxid. Met. vol. 8, no. 4, Aug. 1974, pp. 179-209.

14. Bourhis, Y.; and Saint-John, C.: On the Role of Refractory Elements in the Hot Corrosion of Nickel Base Alloys. Preceedings of the Symposium on Properties of High Temperature Alloys, Z.A. Foroulis and F.S. Pettit, eds., Electrochemical Society, 1977, pp. 595-606.

15. Lowell, Carl E.; and Deadmore, Daniel L.: The Kinetics of High Velocity High-Temperature Corrosion of U-700. Proceedings of the Symposium on Corrosion in Fossil Fuel Systems, I.G. Wright, ed., Electrochemical Society, 1983, pp. 365-394.

16. Santoro, Gilbert J.: Hot Corrosion of Four Superalloys: HA-188, S-57, IN-617, and TD-NiCrAl. Oxid. Met., vol. 13, no. 5, Oct. 1979, pp. 405-435.

17. Hindam, H.; and Whittle, D.P.: Microstructure, Adhesion and Growth Kinetics of Protective Scales on Metals and Alloys. Oxid. Met., vol. 18, no. 5-6, Dec. 1982, pp. 245-284.

18. Floreen, S.; and Kane, R.H.: Effects of Environment on High-Temperature Fatigue Crack Growth in a Superalloy. Metall. Trans. A, vol. 10, no. 11, Nov. 1979, pp. 1745-1751.

19. Fang, W.C.; and Rapp, R.A.: Electrochemical Reactions in a Pure Na_2SO_4 Melt. J. Electrochem. Soc., vol. 130, no. 12, Dec. 1983, pp. 2335-2341.

20. Misra, A.K.; Unpublished Results.

21. Misra, Ajaya K.; and Stearns, Carl A.: Mechanism of Corrosion of Ni Base Superalloys by Molten Na_2MoO_4 at Elevated Temperatures. NASA TM-83580, 1983.

TABLE I. - COMPOSITION
OF THE ALLOY
UDIMET 700

Element	Wt %	At %
Ni	55.32	52.5
Co	17.5	16.4
Cr	14.8	15.8
Al	4.4	9
Ti	2.95	3.3
Mo	5.03	2.8

TABLE II. - RATE DURING THE LINEAR PERIOD OF WEIGHT GAIN AFTER THE BEGINNING OF THE SECOND BREAK-AWAY OXIDATION IN THE INITIAL CORROSION PERIOD FOR THE HEAVIER DOSES OF Na_2SO_4 AT 950 °C

Dose, mg/cm^2	Rate of weight gain, mg/cm^2-hr
3.63	0.764
3.38	.829
5.09	.77
4.36	.765
3.56	.786

TABLE III. - AVERAGE RATE OF WEIGHT GAIN DURING THE INDUCTION PERIOD FOR THE HEAVIER DOSES OF Na_2SO_4 AS A FUNCTION OF THE AMOUNT OF Na_2SO_4 AT 950 °C

Dose, mg/cm^2	Average rate of weight gain during the induction period, mg/cm^2-hr
3.5	0.133
4.36	.225
6.42	.4

TABLE IV. - LENGTH OF INDUCTION PERIOD AT 900 °C AS A FUNCTION OF THE AMOUNT OF Na_2SO_4

Amount of Na_2SO_4, mg/cm^2	Length of the induction period, hr
0.3	10
0.5	10
0.73	90
1.47	300
5	100

TABLE V. - TOTAL AMOUNT OF SO_2 EVOLVED DURING THE PERIOD OF ACCELERATING CORROSION AS A FUNCTION OF THE AMOUNT OF Na_2SO_4 AT 950 °C

Dose, mg/cm^2	Total amount of SO_2 evolved, mmol
2.5	0.065
3.5	.078
4.5	.105
5.7	.16

TABLE VI. - SO_4 CONTENT OF THE WATER-WASHED SOLUTION FOR VARIOUS DOSES OF Na_2SO_4 AT THE END OF THE FIRST BREAKAWAY OXIDATION IN THE INITIAL PERIOD OF CORROSION AT 950 °C

Dose, mg/cm^2	SO_4 in the solution, mmol
0.5	not detectable
0.9	not detectable
1.3	0.0007
1.8	0.015
3.5	0.1245

TABLE VII. - SO_4 CONTENT OF THE WATER-WASHED SOLUTION AFTER 4 HR OF CORROSION AT 950 °C FOR THE HEAVIER DOSES OF Na_2SO_4

Dose, mg/cm^2	SO_4 in the solution, mmol
3.5	0.054
3.8	.049
4.5	.051
5.7	.049

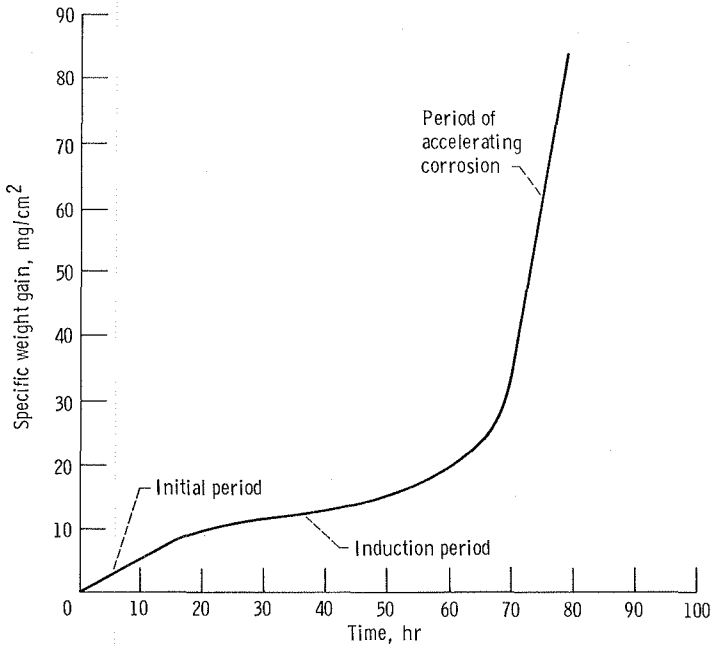

Figure 1. - Corrosion kinetics for U-700, coated with 3.5 mg/cm^2 Na_2SO_4 and oxidized at 950 °C.

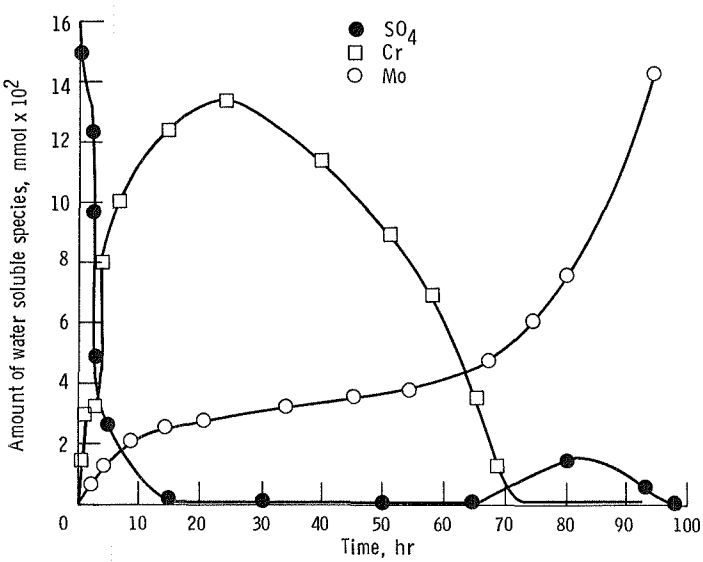

Figure 2. - Amount of water soluble species as a function of time for U-700, coated with 3.5 mg/cm^2 Na_2SO_4 and corroded at 950 °C.

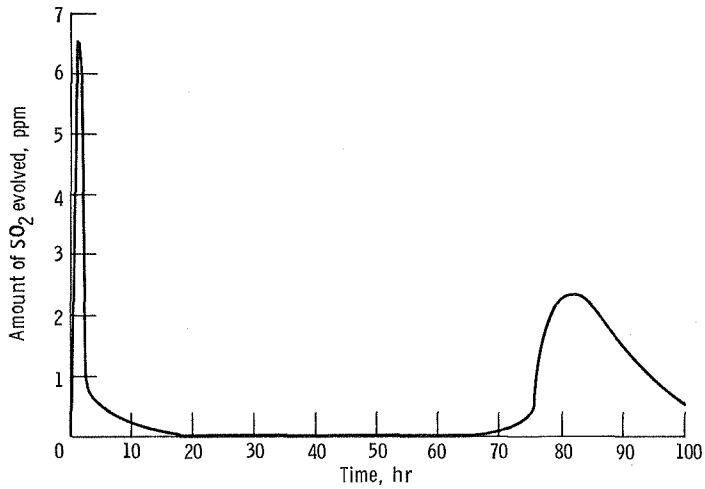

Figure 3. - SO_2 evolution as a function of time for U-700, coated with 3.5 mg/cm^2 Na_2SO_4 and corroded at 950 ^{0}C.

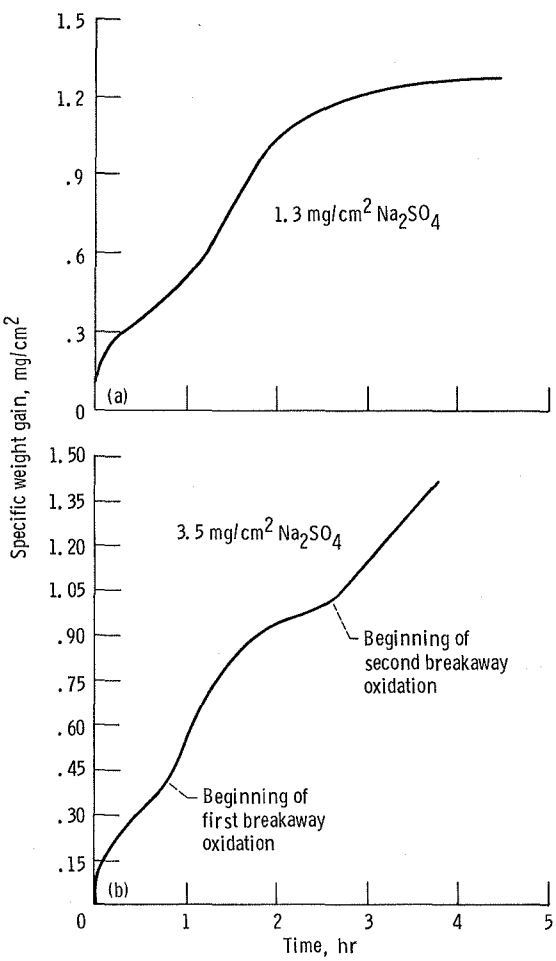

Figure 4. - Corrosion kinetics during the first 4-hr of corrosion for U-700, coated with different doses of Na_2SO_4 and corroded at 950 ^{0}C.

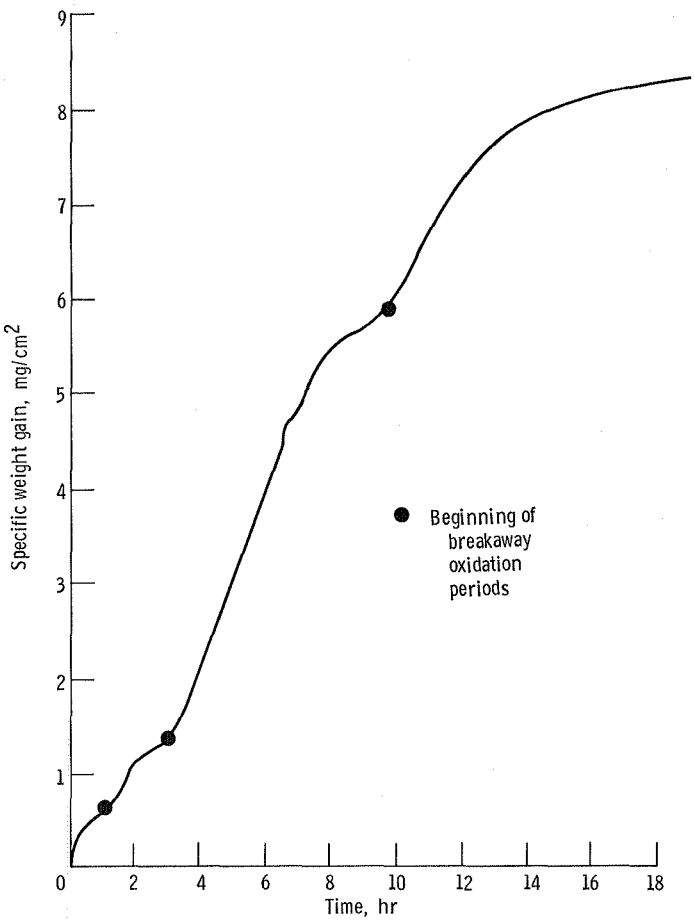

Figure 5. - Details of the corrosion kinetics during the initial period for U-700, coated with 3.5 mg/cm^2 Na_2SO_4 and corroded at 950 ^{0}C.

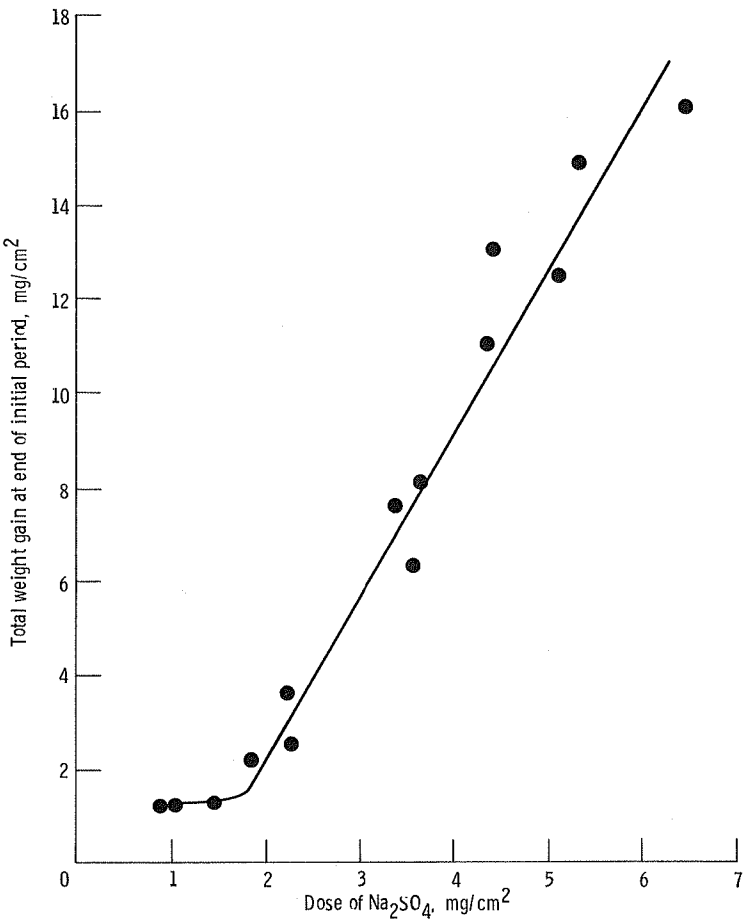

Figure 6. - Total weight gain at the end of the initial period as a function of the amount of Na_2SO_4 for U-700, corroded at 950 ^{0}C.

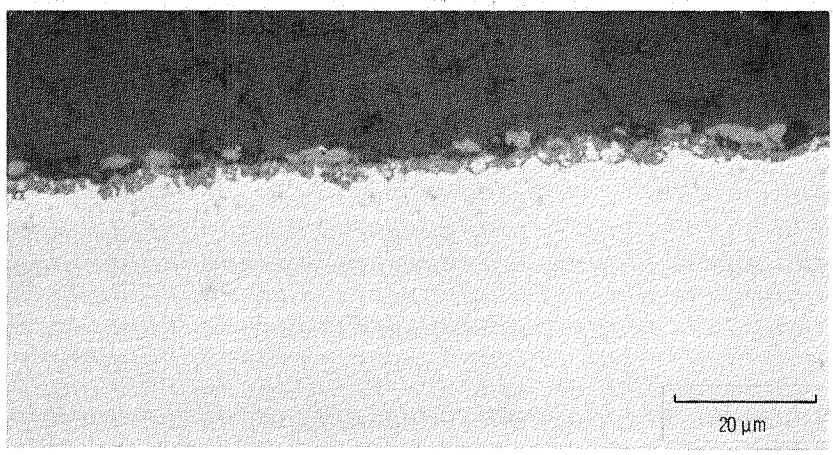

(a) After 15 min of corrosion.

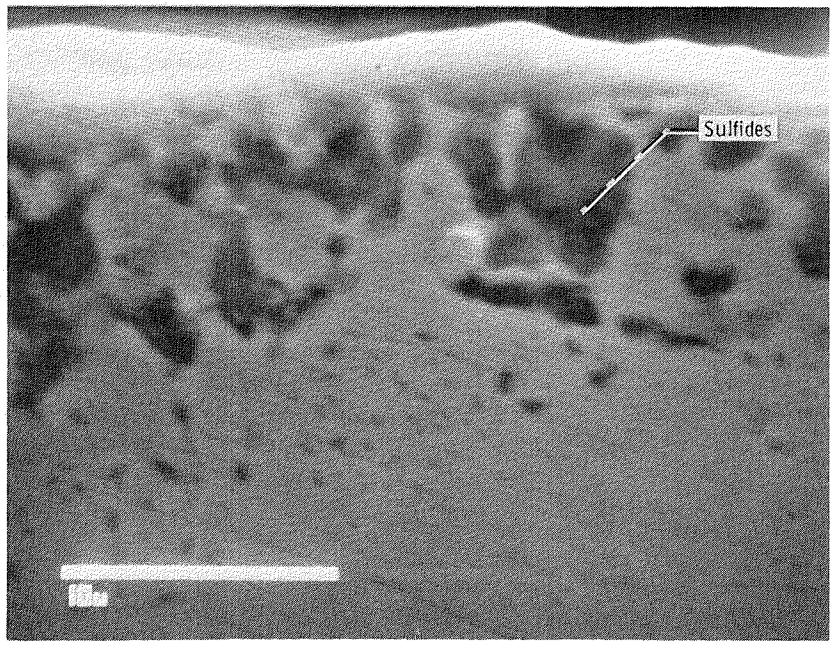

(b) At the beginning of the first breakaway oxidation period.

Figure 7. - Scale morphology for U-700, coated with 3.5 mg/cm^2 Na_2SO_4 and corroded for different times during the initial period at 950 ^{0}C.

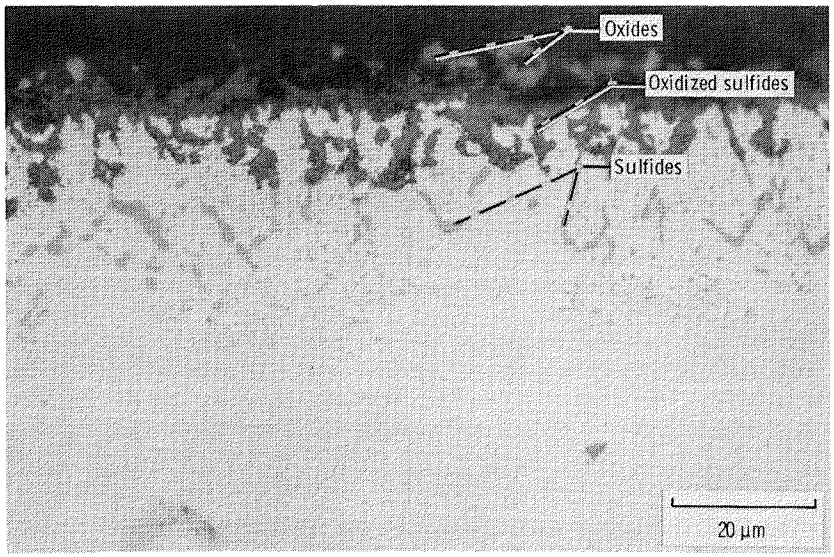

(c) At the end of the first breakaway oxidation period. Note: The lighter internal particles are sulfides and the dark internal particles are oxides.

Figure 7. - Concluded.

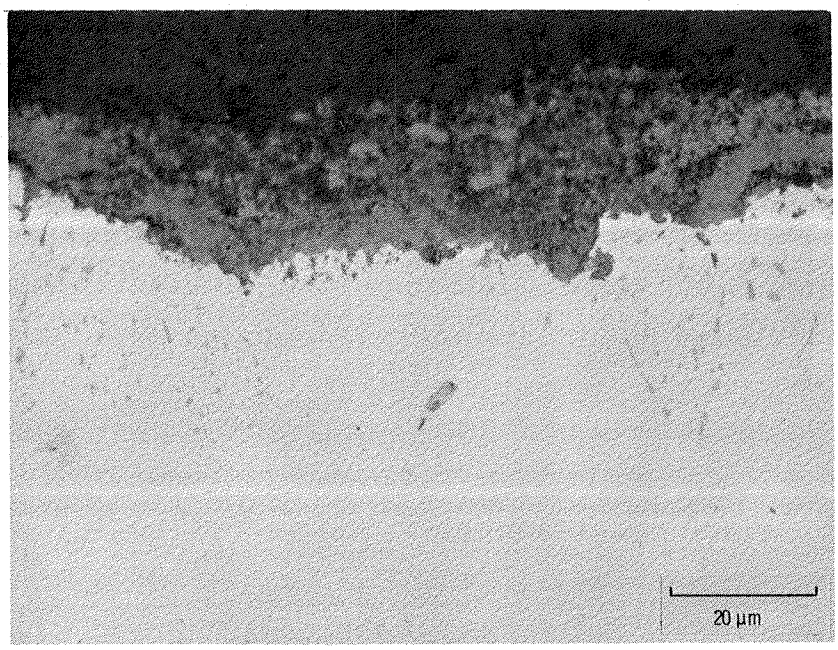

Figure 8. - Scale morphology during the induction period for low and intermediate doses of Na_2SO_4 (< 2 mg/cm^2) for U-700, corroded at 950 °C.

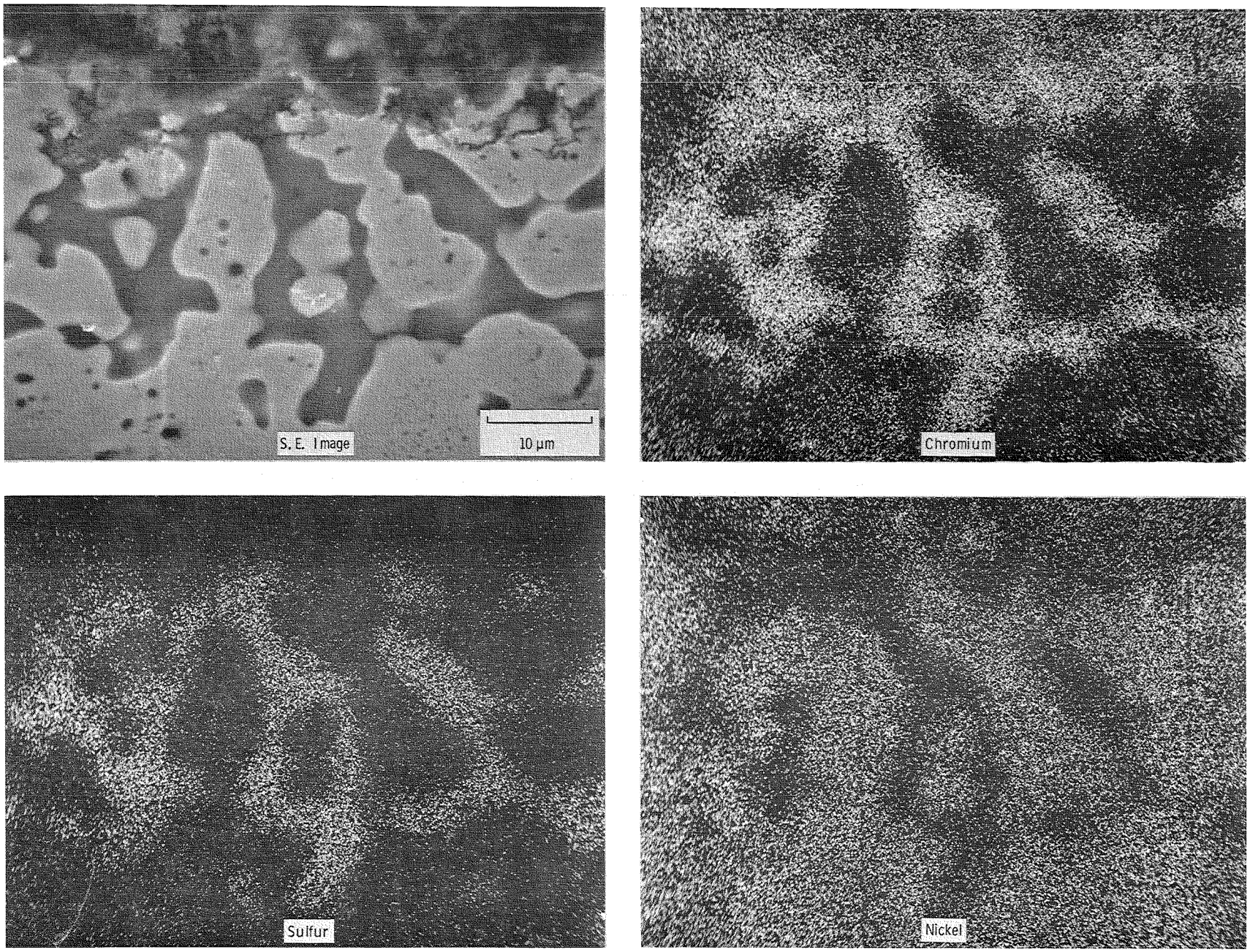

(a) S. E. image and x-ray maps.

Figure 9. - Scale morphology at the beginning of the second breakaway oxidation in the corrosion kinetics in the initial period for U-700, coated with 3.5 mg/cm^2 Na_2SO_4 and corroded at 950 ^{o}C.

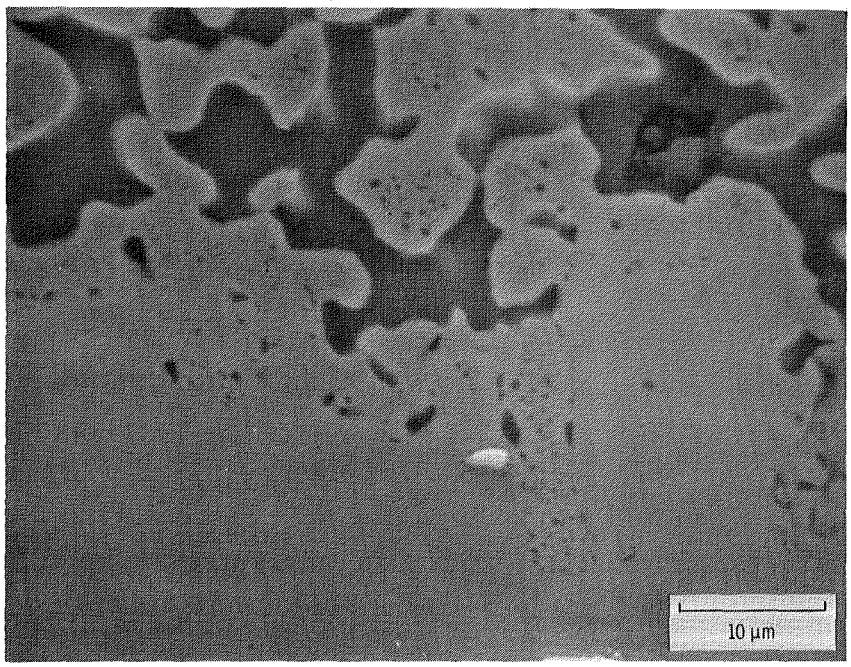

(b) Details of the interface.

Figure 9. - Concluded.

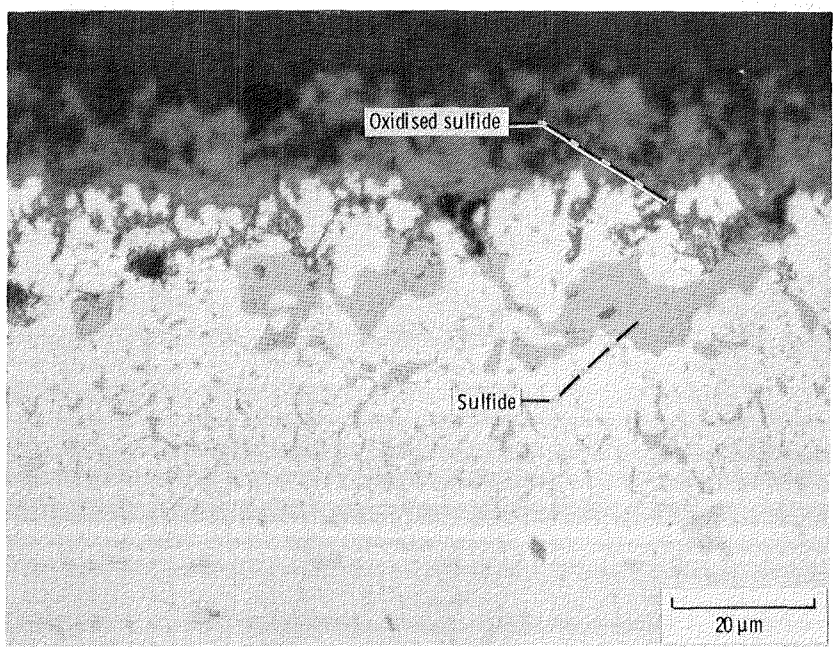

(a) After 1 hr from the beginning of the second breakaway oxidation.

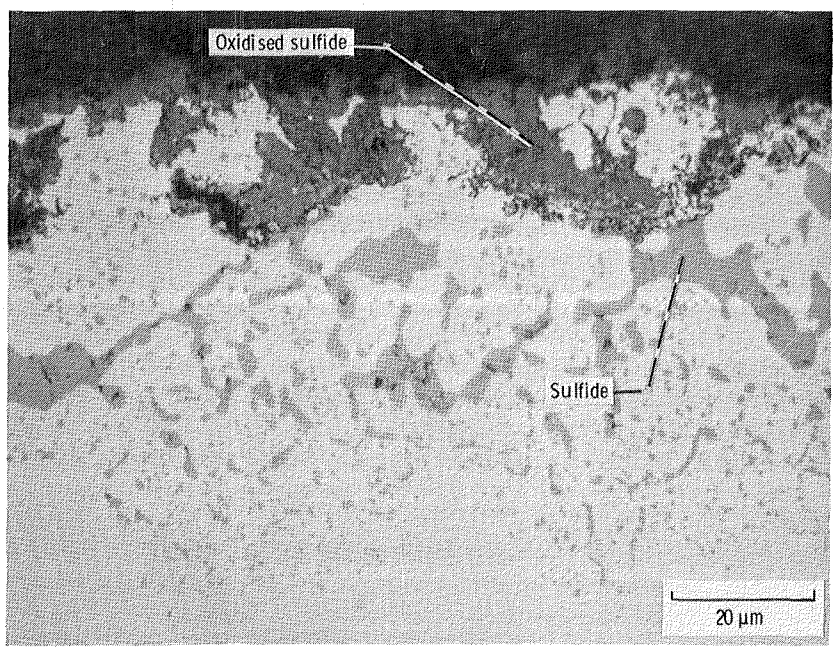

(b) After 5 hr from the beginning of the second breakaway oxidation.

Figure 10. - Scale morphology during the period of linear weight gain after the second breakaway oxidation in the initial corrosion kinetics for U-700, coated with 3.5 mg/cm^2 Na_2SO_4 and corroded at 950 ^{0}C.

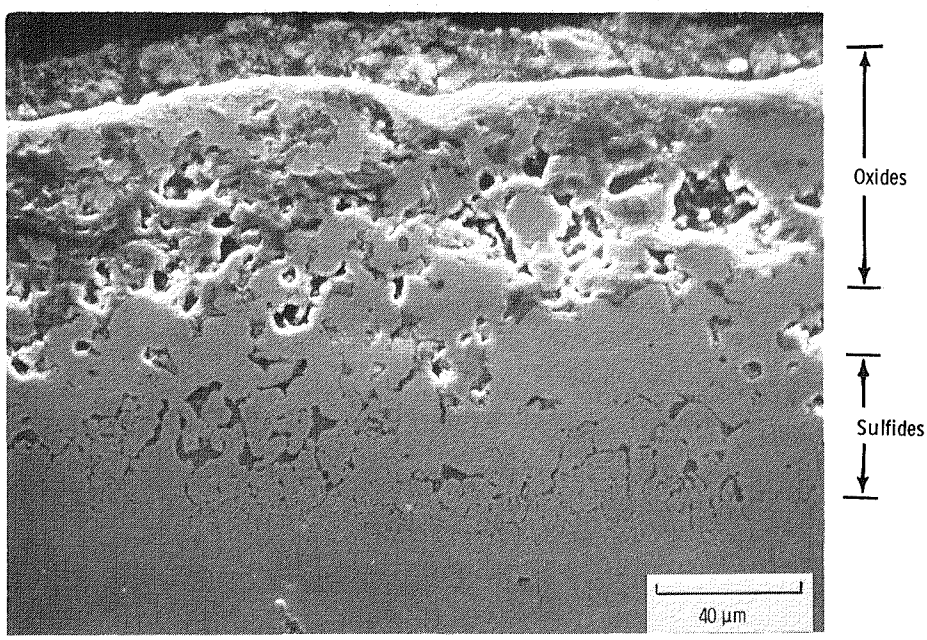

(a) Cross section.

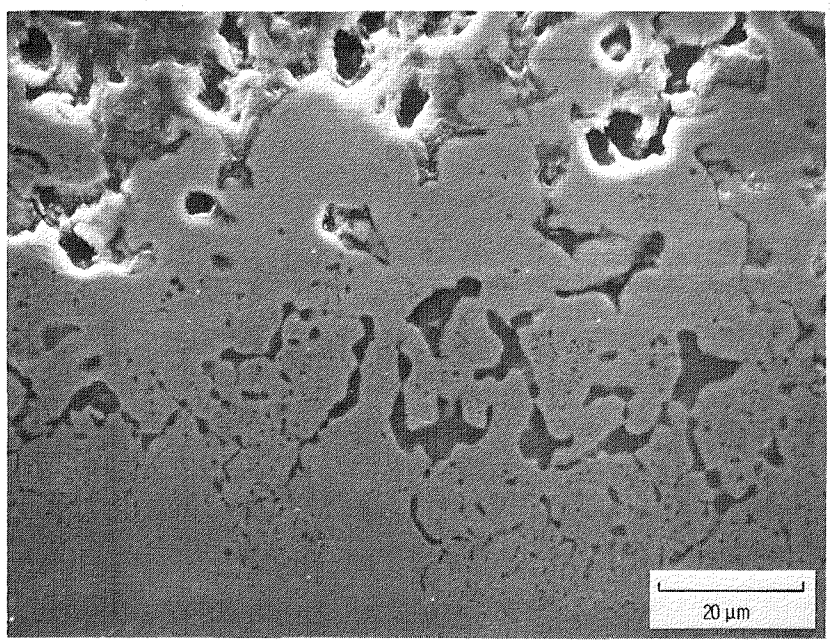

(b) Details of the scale-metal interface.

Figure 11. - Typical scale morphology at the end of the initial period of corrosion at 950 ^{0}C for U-700, coated with heavy dose of Na_2SO_4 (> 3 mg/cm^2).

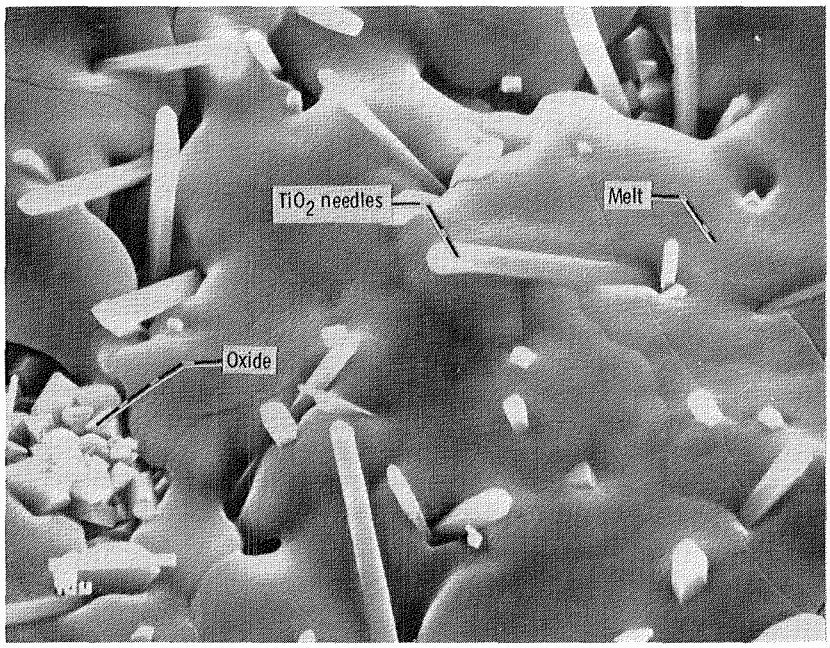

(a) After 15 min.

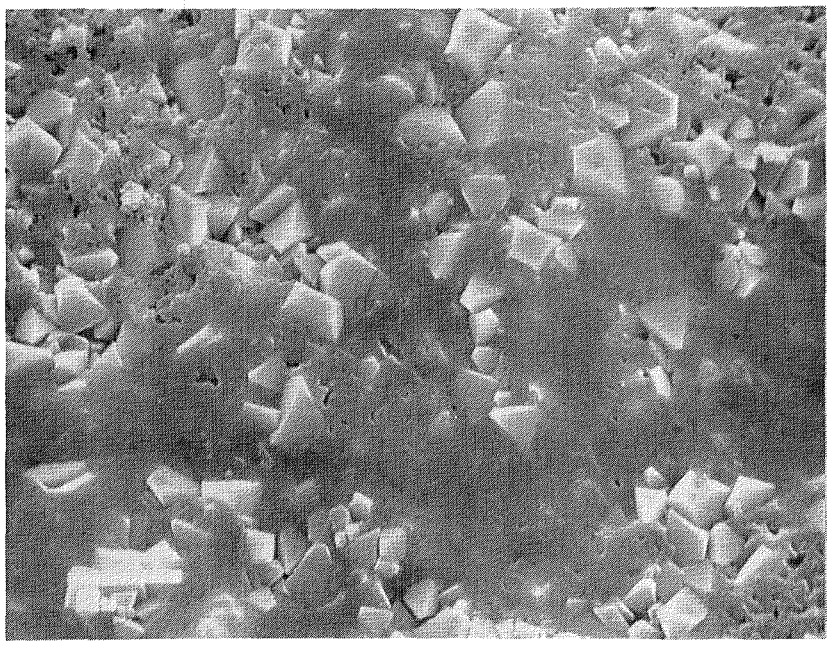

(b) After 30 min.

Figure 12. - Top surface of U-700, coated with Na_2SO_4 and corroded at 950 ^{o}C for different lengths of time.

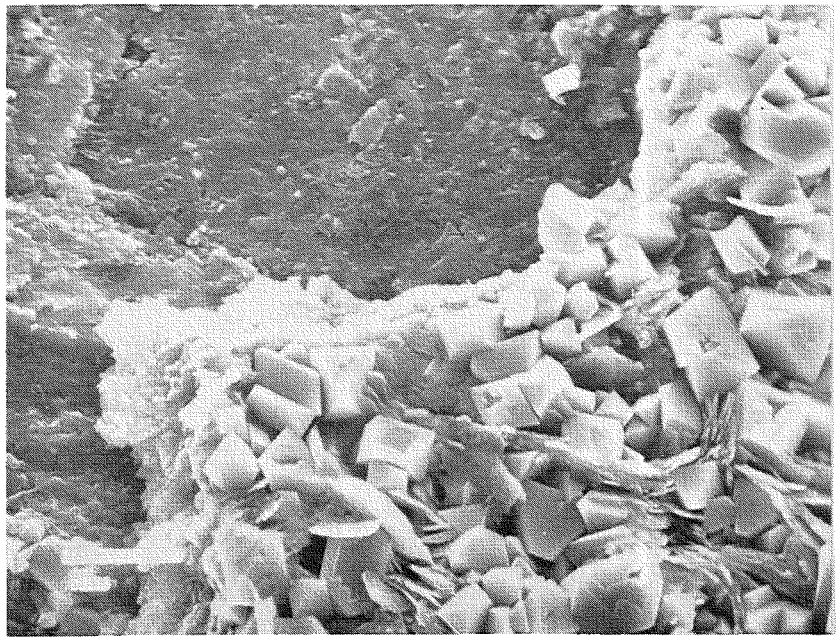

(a) Overall view.

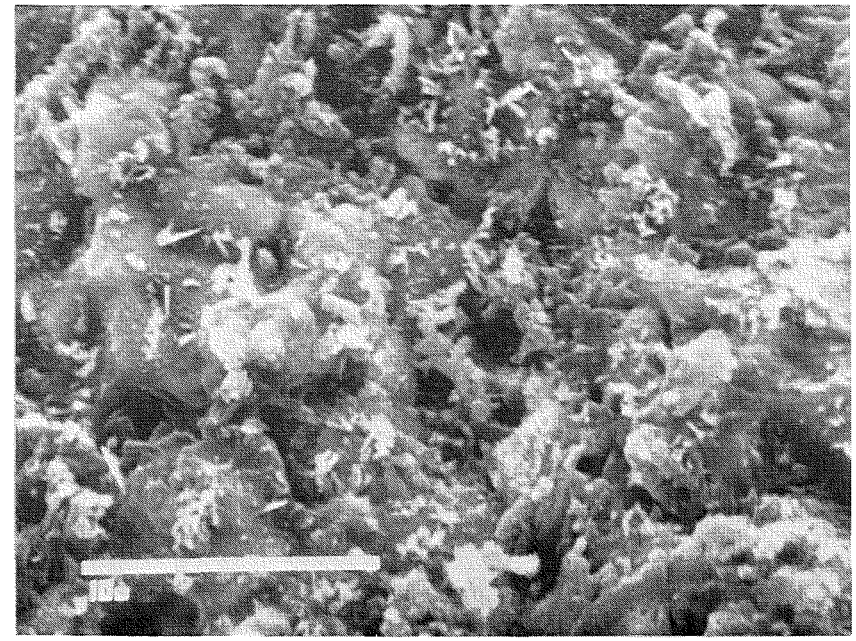

(b) Details of the region, where the outer oxide has spalled off the surface.

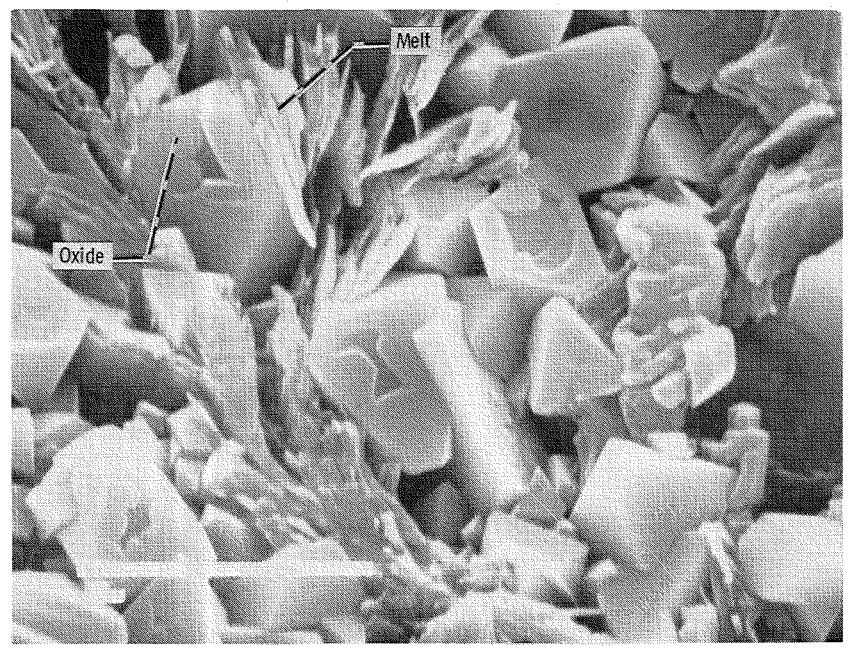

(c) Details of the outer oxide layer.

Figure 13. - Top surface of U-700, coated with Na_2SO_4 and corroded at 950 ^{o}C for 1 hr.

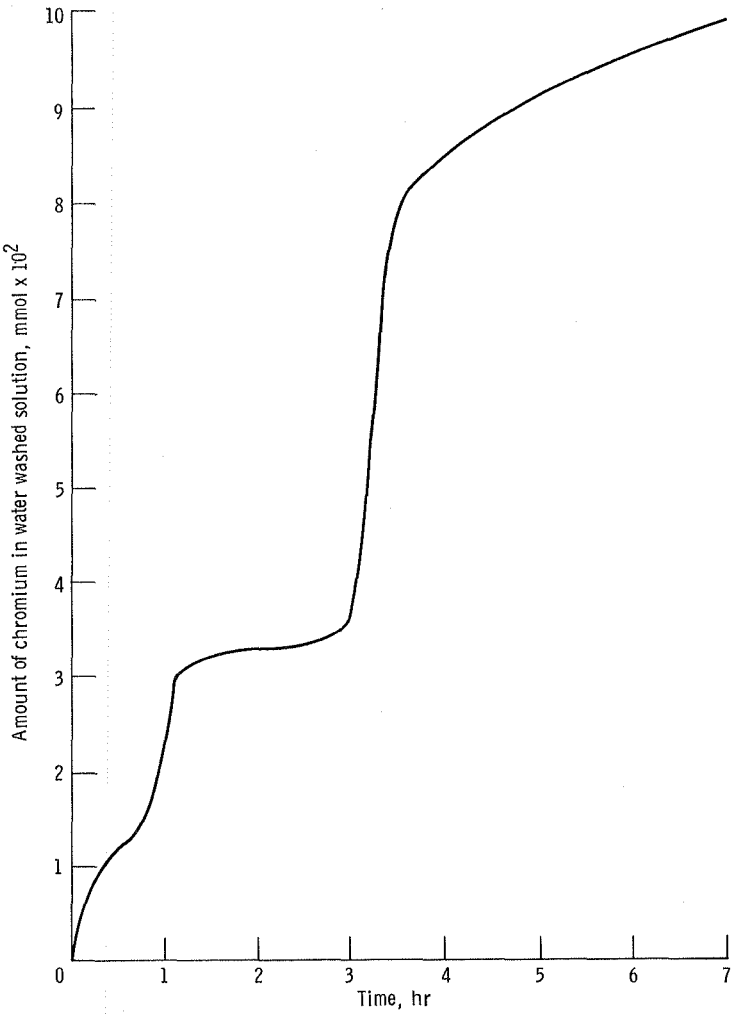

Figure 14. - Cr content of water-washed solution as a function of time during initial period for U-700, coated with 3.5 mg/cm^2 Na_2SO_4 and corroded at 950 ^{0}C.

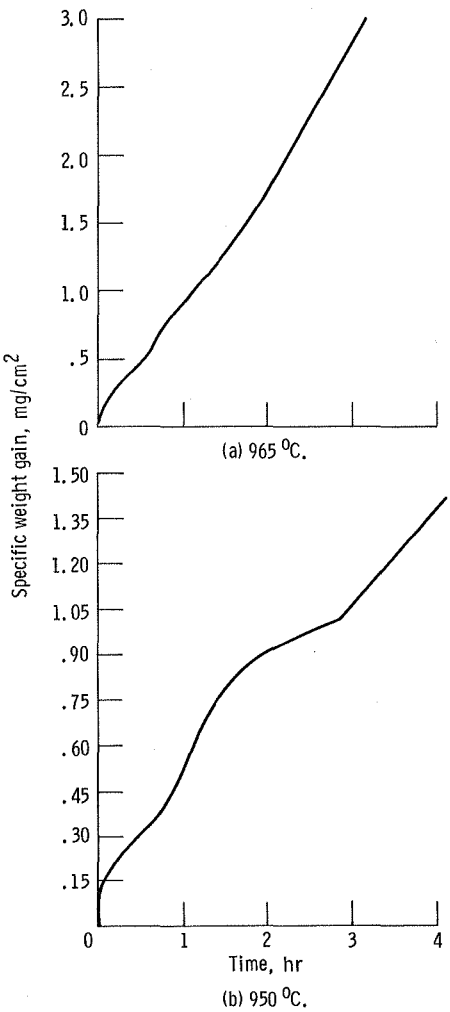

Figure 15. - Corrosion kinetics during initial period as a function of temperature for U-700, coated with 3.5 mg/cm^2 Na_2SO_4.

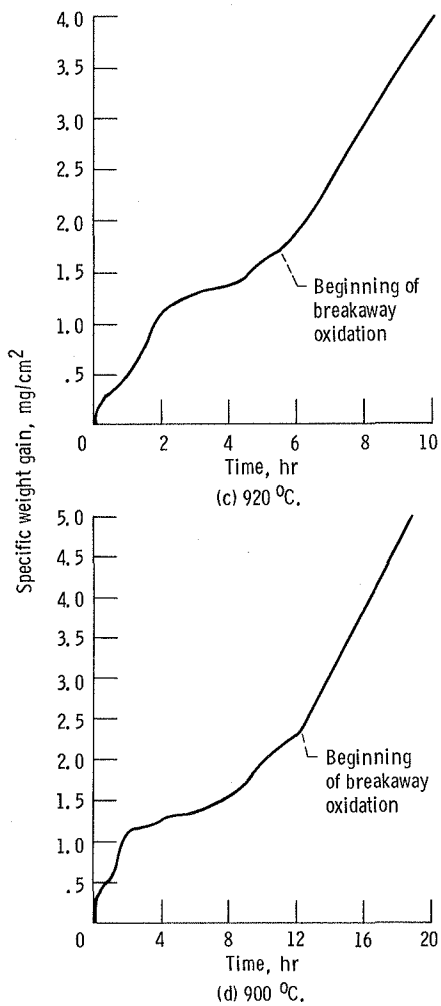

Figure 15. - Concluded.

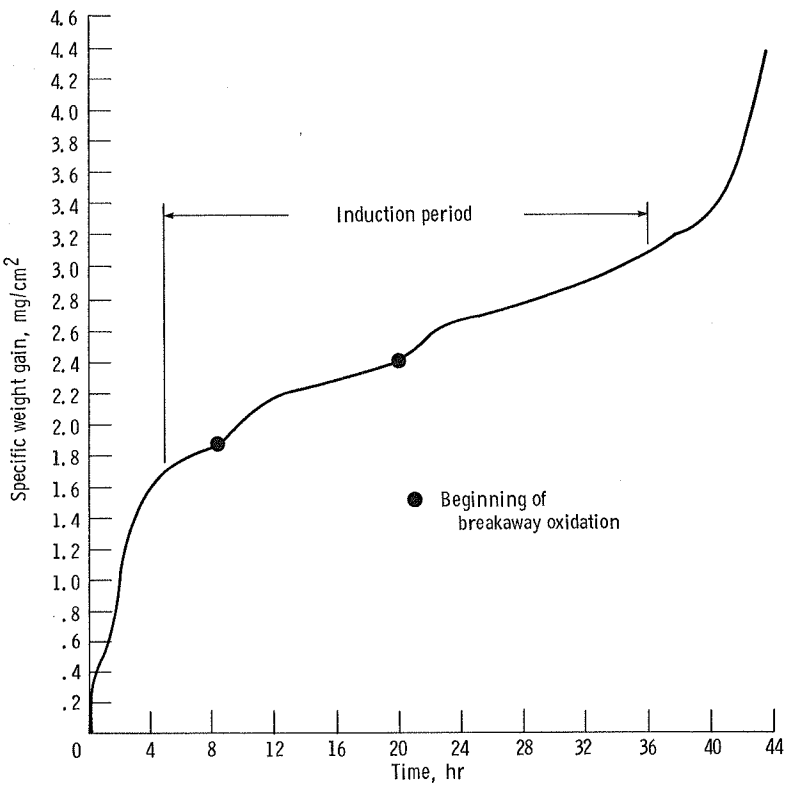

Figure 16. - Details of kinetics during induction period for U-700, coated with 1.3 mg/cm^2 Na_2SO_4 and corroded at 950 ^{0}C.

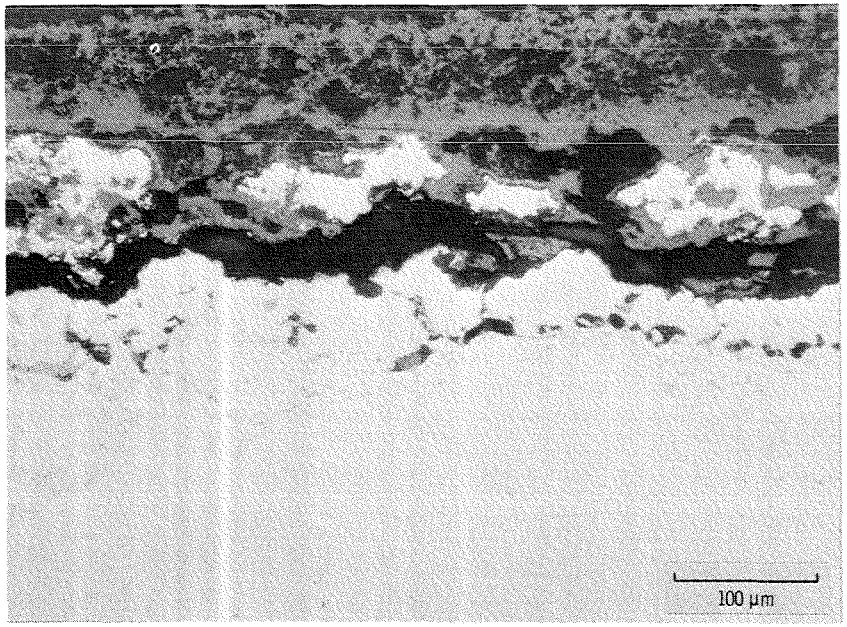

(a) Cross section.

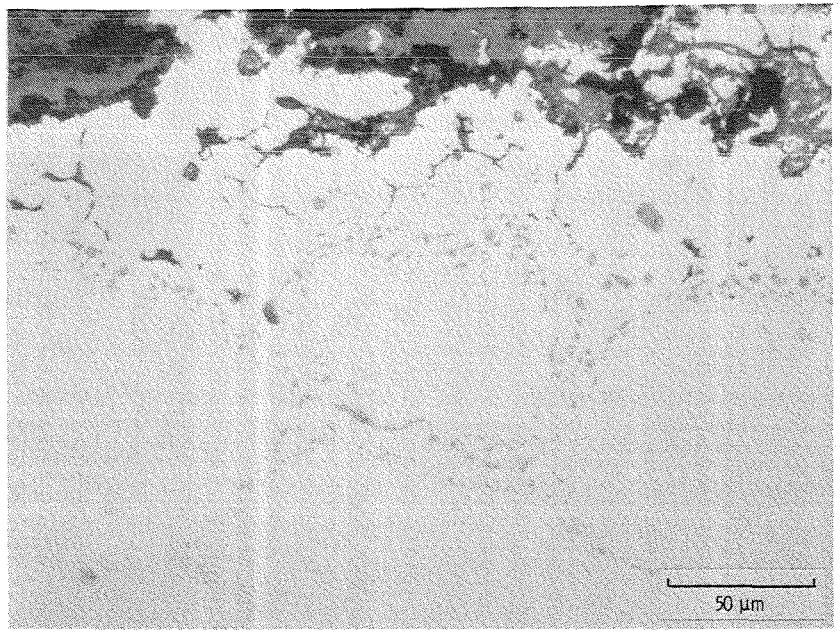

(b) Details of the scale-metal interface.

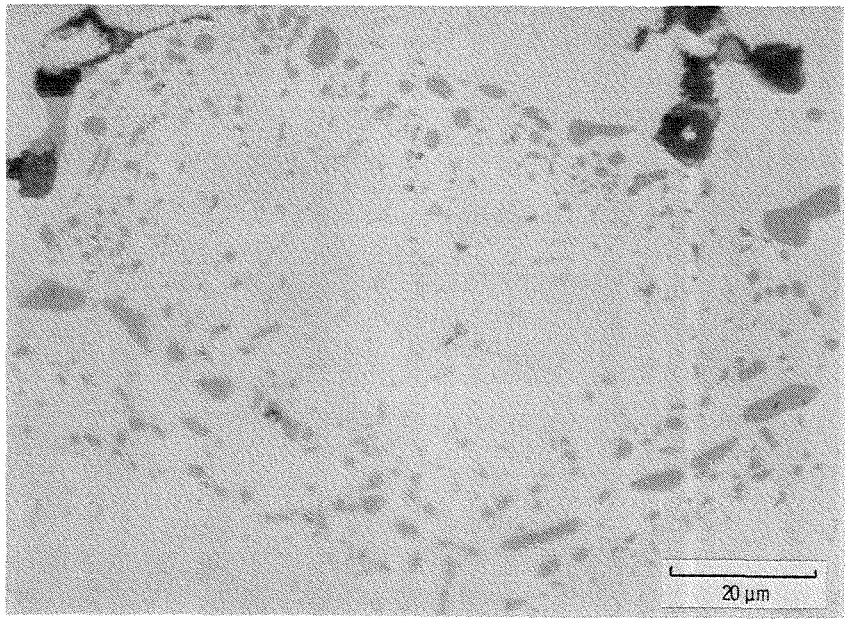

(c) Details of the grain boundary sulfides.

Figure 17. - Typical scale morphology during the induction period for the heavier doses of Na_2SO_4 (> 3 mg/cm^2) for U-700, corroded at 950 ^{0}C.

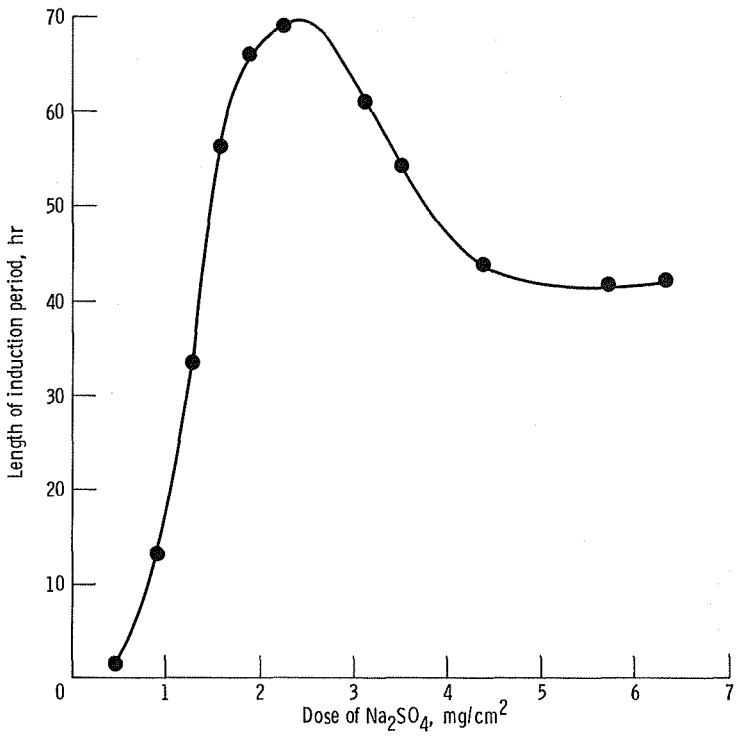

Figure 18. - Length of induction period as a function of amount of Na_2SO_4 for U-700 at 950 ^{0}C.

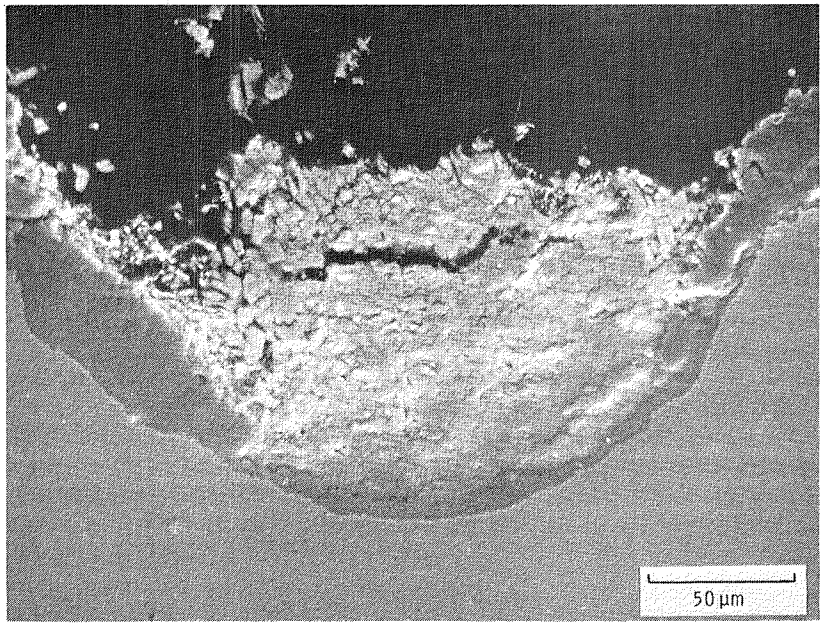

(a) S. E. image.

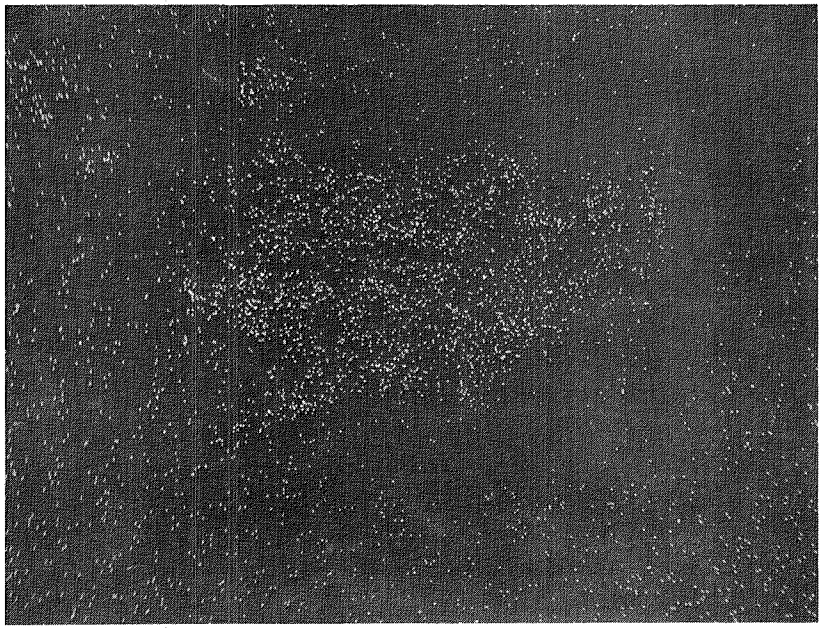

(b) Molybdenum x-ray map.

Figure 19. - Typical scale morphology at the end of the period of accelerating corrosion for U-700.

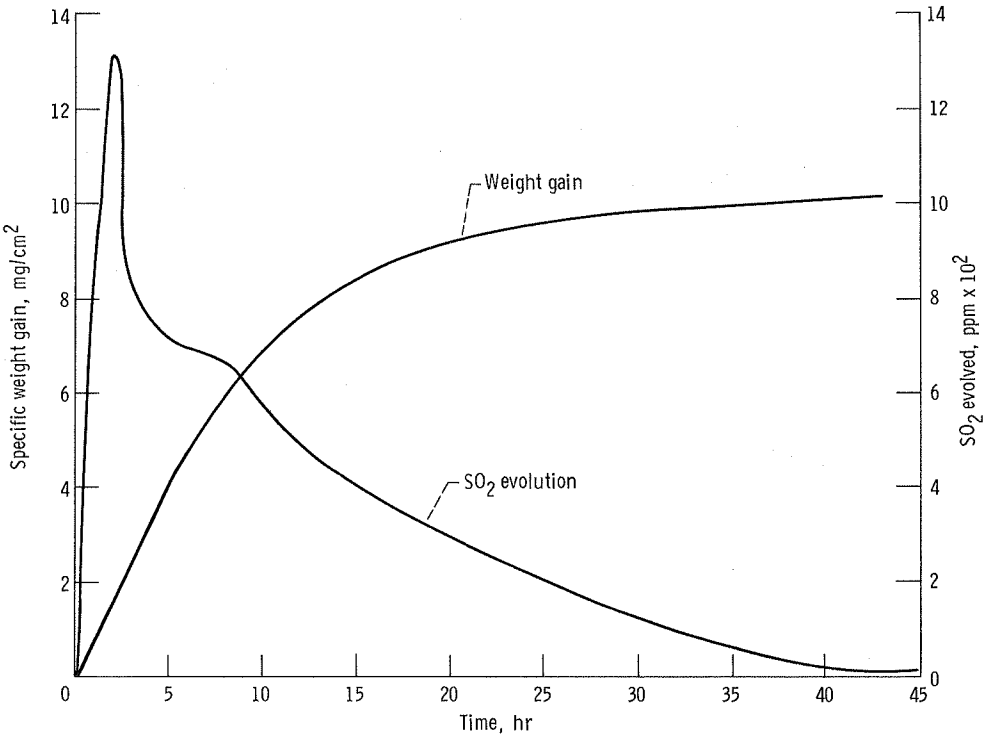

Figure 20. - Kinetics and SO_2 evolution for U-700, coated with 5.7 mg/cm^2 Na_2SO_4 and corroded at 950 °C until the beginning of second breakaway oxidation period, then washed in hot distilled water and reoxidized again at 950 °C.

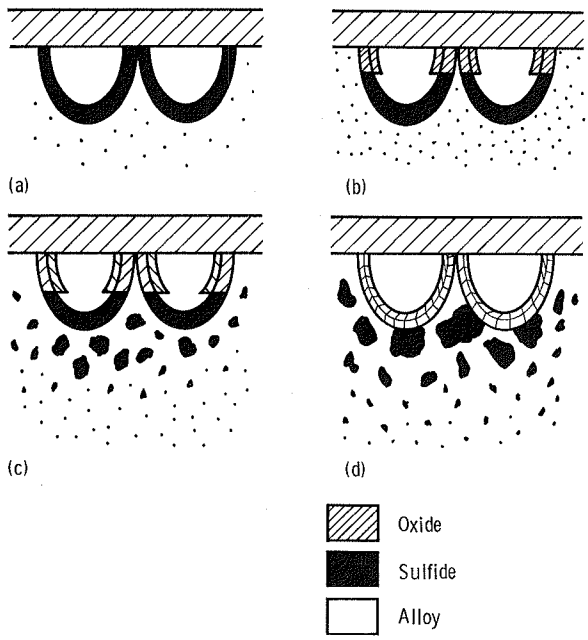

Figure 21. - A generalized model for degradation due to formation of sulfides.

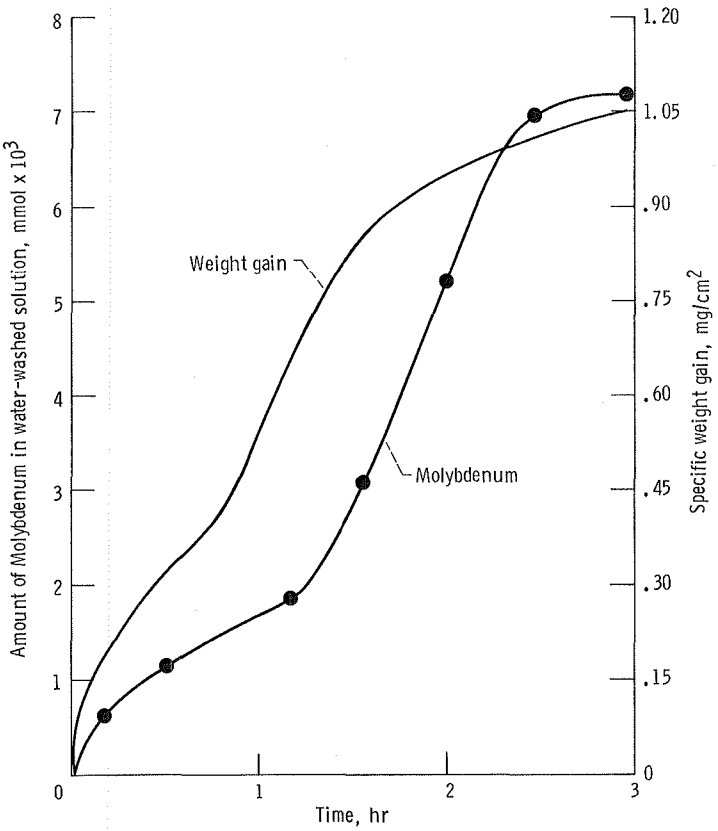

Figure 22. - Molybdenum content of water-washed solution during first 3-hr of corrosion for U-700, coated with 1.5 mg/cm^2 Na_2SO_4 and oxidized at 950 ^{o}C.

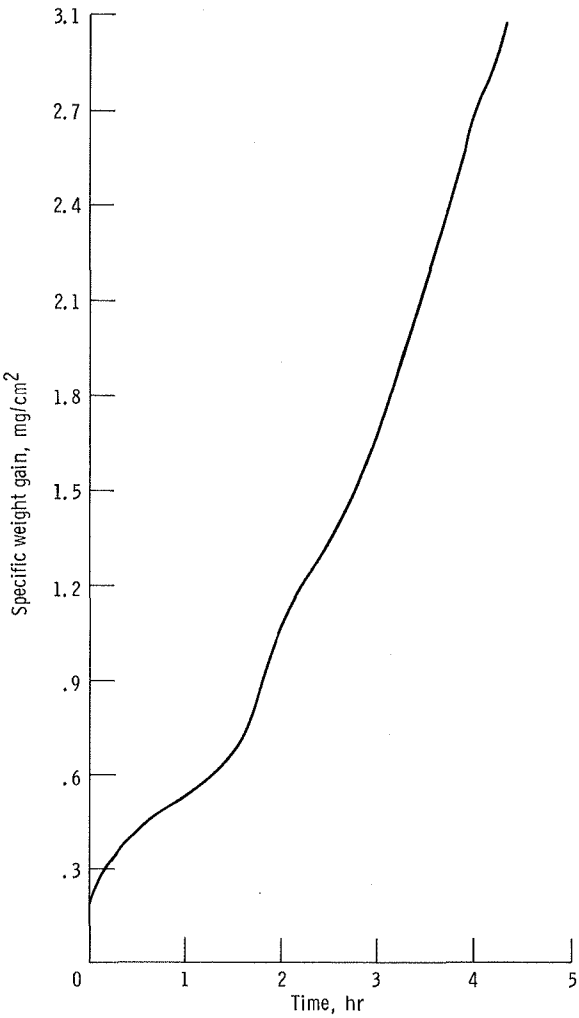

Figure 23. - Kinetics of corrosion for U-700, coated with 0.5 mg/cm^2 Na_2SO_4 and oxidized at 950 ^{0}C.

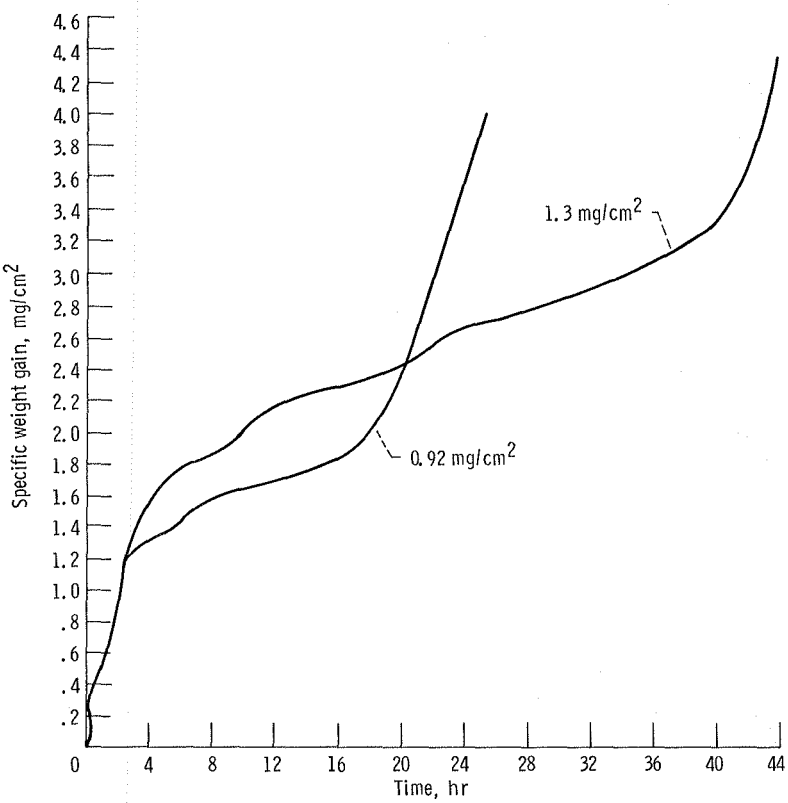

Figure 24. - A comparison of corrosion kinetics for U-700, coated with two different doses of Na_2SO_4 (0.92 and 1.3 mg/cm^2) and oxidized at 950 ^{0}C.

1. Report No.	2. Government Accession No.	3. Recipient's Catalog No.
NASA TM-86882		

4. Title and Subtitle	5. Report Date
Studies on the Hot Corrosion of a Nickel-Base Superalloy - Udimet 700	November 1984
	6. Performing Organization Code: 533-04-1E
7. Author(s): Ajay K. Misra	8. Performing Organization Report No.: E-2314
	10. Work Unit No.
9. Performing Organization Name and Address: National Aeronautics and Space Administration, Lewis Research Center, Cleveland, Ohio 44135	11. Contract or Grant No.
	13. Type of Report and Period Covered: Technical Memorandum
12. Sponsoring Agency Name and Address: National Aeronautics and Space Administration, Washington, D.C. 20546	14. Sponsoring Agency Code

15. Supplementary Notes

Ajay K. Misra, Case Western Reserve University, Dept. of Metallurgy and Materials Science, Cleveland, Ohio and NASA Lewis Resident Research Associate (work performed under NASA Grant NCC 3-43).

16. Abstract

The hot corrosion of a nickel-base superalloy, Udimet 700, has been studied in the temperature range of 884 to 965 °C and with different amounts of Na_2SO_4. Two different modes of degradation were identified: (1) formation of Na_2MoO_4 - MoO_3 melt and fluxing by this melt, (2) formation of large interconnected sulfides. The present studies have shown that the dissolution of Cr_2O_3, TiO_2 in the Na_2SO_4 melt does not play a significant role in the overall corrosion process. The conditions for the formation of massive interconnected sulfides were identified and a mechanism of degradation due to sulfide formation is described. The formation of Na_2MoO_4 - MoO_3 melt requires an induction period and various physicochemical processes during the induction period were identified. The factors affecting the length of the induction period were also examined. From the present studies, the melt penetration through the oxide appears to be the prime mode of degradation whether the degradation is due to the formation of sulfides or the formation of the Na_2MoO_4 - MoO_3 melt.

17. Key Words (Suggested by Author(s))	18. Distribution Statement
Nickel-base superalloy Hot corrosion Sulfides Sodium sulfate	Unclassified - unlimited STAR Category 26

19. Security Classif. (of this report)	20. Security Classif. (of this page)	21. No. of pages	22. Price*
Unclassified	Unclassified		

*For sale by the National Technical Information Service, Springfield, Virginia 22161

End of Document